

A TUNGSTEN-RICH PORPHYRY MOLYBDENUM OCCURRENCE AT BEAR MOUNTAIN,
NORTHEAST ALASKA

by James C. Barker and R. C. Swainbank

***** Open file report 8-85

TN) STATES DEPARTMENT OF THE INTERIOR
23
.U44 am P. Clark, Secretary
85-8
c.3

U OF MINES

t C. Horton, Director



**James Boyd
Memorial Library**

**UNITED STATES
BUREAU OF MINES**



**JAMES BOYD
MEMORIAL LIBRARY**

*** PREFACE

Strategic and critical minerals are essential materials for which no satisfactory substitutes exist. The United States is dependent upon foreign sources of many minerals needed for industry and defense. The Bureau of Mines, as part of its mission to ensure an adequate supply of minerals to meet the Nation's needs, is currently reviewing and making an inventory of occurrences of strategic and critical minerals in Alaska. The Bear Mountain study is one of numerous site investigations by the Bureau's Alaska Field Operations Center.

Alaska may contain deposits of certain strategic and critical minerals not found in economic quantities elsewhere in the United States. If recoverable resources of these minerals can be demonstrated to occur in Alaska, then their existence serves as an in-the-ground stockpile that could be developed should foreign sources be threatened or curtailed. Thus, the present economic viability of a deposit or its land status classification need not be essential criteria in considering the strategic availability of a mineral resource.

CONTENTS

	<u>Page</u>
Abstract.....	8
Introduction.....	9
Acknowledgments.....	10
Procedure.....	11
Regional geology.....	14
Local geology.....	16
Surficial geology.....	16
Lithology.....	17
Structure.....	21
Age relationships.....	22
Alteration.....	23
Geophysics.....	27
Radiometric survey.....	27
VLF-EM survey.....	28
Geochemistry.....	29
Placer mineralization.....	31
Lode mineralization.....	33
Discussion.....	36
Conclusion.....	39
References.....	42
Appendix A.--Soil samples and analytical results.....	45
Appendix B.--Rock sample descriptions and analytical results.....	51
Appendix C.--VLF-EM radiometric measurements.....	55

ILLUSTRATIONS

Follows Page

1. Index map of northern Alaska showing location of report area.	9
2. Regional geology of the Bear Mountain area.....	9
3. Survey grid and sample location map.....	11
4. View looking southeast showing the surficial geology.....	17
5. Local geology.....	17
6. Intrusive breccia near grid station 1000E - 600S.....	20
7. Intrusive phases of the subvolcanic complex.....	24
8. Interpretative contouring of total-count radiometric values in counts per second.....	27
9. VLF-EM survey map.....	28
10. Cumulative frequency histograms of soil metal values (lead, molybdenum, and tungsten).....	30
11. Distribution of molybdenum in soils.....	30
12. Distribution of tungsten in soils.....	30
13. Distribution of lead in soils.....	30
14. Distribution of niobium in soils.....	30
15. Zonation of lead, molybdenum, and tungsten expressed as a percentage of total metal content in soils.....	31

TABLES

	<u>Page</u>
1. Quantitative analytical procedures and detection limits....	13
2. Alluvial heavy mineral concentrates.....	32

UNIT OF MEASURE ABBREVIATIONS USED IN THIS REPORT

cps	counts per second	m.y.	million years
ft	foot	pct	percent
g	gram	ppm	parts per million
in	inch	yd ³	cubic yard
lb	pound		

A TUNGSTEN-RICH PORPHYRY MOLYBDENUM OCCURRENCE AT BEAR MOUNTAIN,
NORTHEAST ALASKA

By James C. Barker¹ and R. C. Swainbank²

*** ABSTRACT

In 1983, the Bureau of Mines investigated an occurrence of molybdenum and tungsten near Bear Mountain in northeastern Alaska. A mineralized area defined by greater than 600 ppm molybdenum in soils over approximately 100 acres is underlain by an altered complex of rhyolite porphyry, quartz porphyry, intrusive breccia, and rhyolite porphyry dikes. Soil with at least 500 ppm tungsten also defines an area partially coincident with the molybdenum area. These values are approximately equivalent to 0.1 pct MoS₂ and 0.06 pct WO₃. Soil samples also indicate low-grade niobium (columbium) enrichment. Rock samples from the Bear Mountain occurrence contained 0.1 to 0.8 pct molybdenum and 0.06 to 0.6 pct tungsten. Although sulfide minerals have been leached, the tungsten mineral wolframite, comprising both the huebnerite and ferberite end members was identified in rocks and placer concentrates. Zonation between a higher-level, wolframite-topaz zone and a lower-level central molybdenum-rich gossan zone with lower tungsten values is evident.

Bear Mountain occurs within a regional east-west structural trend of small domes, intrusions, and doubly-plunging anticlines. This trend can be traced from 50 miles west of Table Mountain, easterly to Ammerman Mountain and beyond into Canada, and is recommended for further evaluation.

¹Supervisory physical scientist, Alaska Field Operations Center, Bureau of Mines, Fairbanks, AK.

²Geologist, Geoprize, Ltd., Fairbanks, AK.

*** INTRODUCTION

Bear Mountain is located on the southern flank of the Brooks Range near the headwaters of the Coleen River in the U.S. Geological Survey (USGS) Table Mountain 1:63,360 (B-2) Quadrangle in northeast Alaska (fig. 1). There is no habitation within a 100-mile radius nor is there overland access to this area. Bear Mountain lies within the National Arctic Wildlife Range, administered by the U.S. Fish and Wildlife Service and closed to mineral entry.

Very little is known about the geology and mineral resources of this remote region of Alaska. Attention was originally drawn to the area in the 1950's by Mr. Ed Owens, a local prospector, who discovered lead and zinc vein mineralization near Galena Creek (fig. 2). In 1968, Brosge' released 1:250,000 scale maps depicting results of geochemical sampling (7).³ Included among those results were two stream sediment

³Underlined numbers in parentheses refer to items in the list of references preceding the appendixes.

samples and a soil sample taken from a valley on the south side of Bear Mountain. These were reported as anomalous in molybdenum, lead, and tungsten, and on the basis of these samples, the possibility of porphyry mineralization was suggested (10). Reconnaissance-level geological mapping at 1:200,000 scale compiled by Brosge' and others in 1976 (11) defined the approximate outline of the Bear Mountain pluton and a nearby small stock. In 1976, Brosge' and the (Bureau) author jointly visited the area of the 1968 geochemical anomalies and examined nearby galena and sphalerite veins at Galena Creek (fig. 2) (9). During that visit they also determined that a porphyry-like body was the likely source of

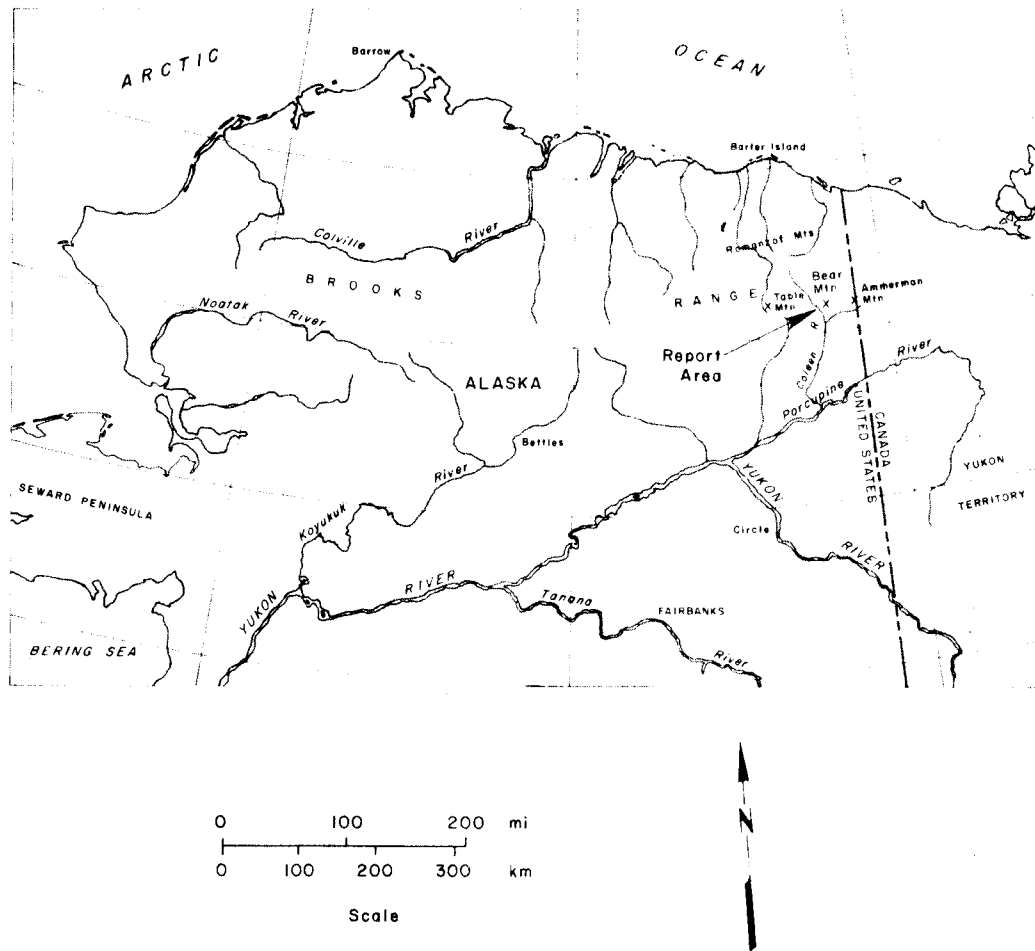
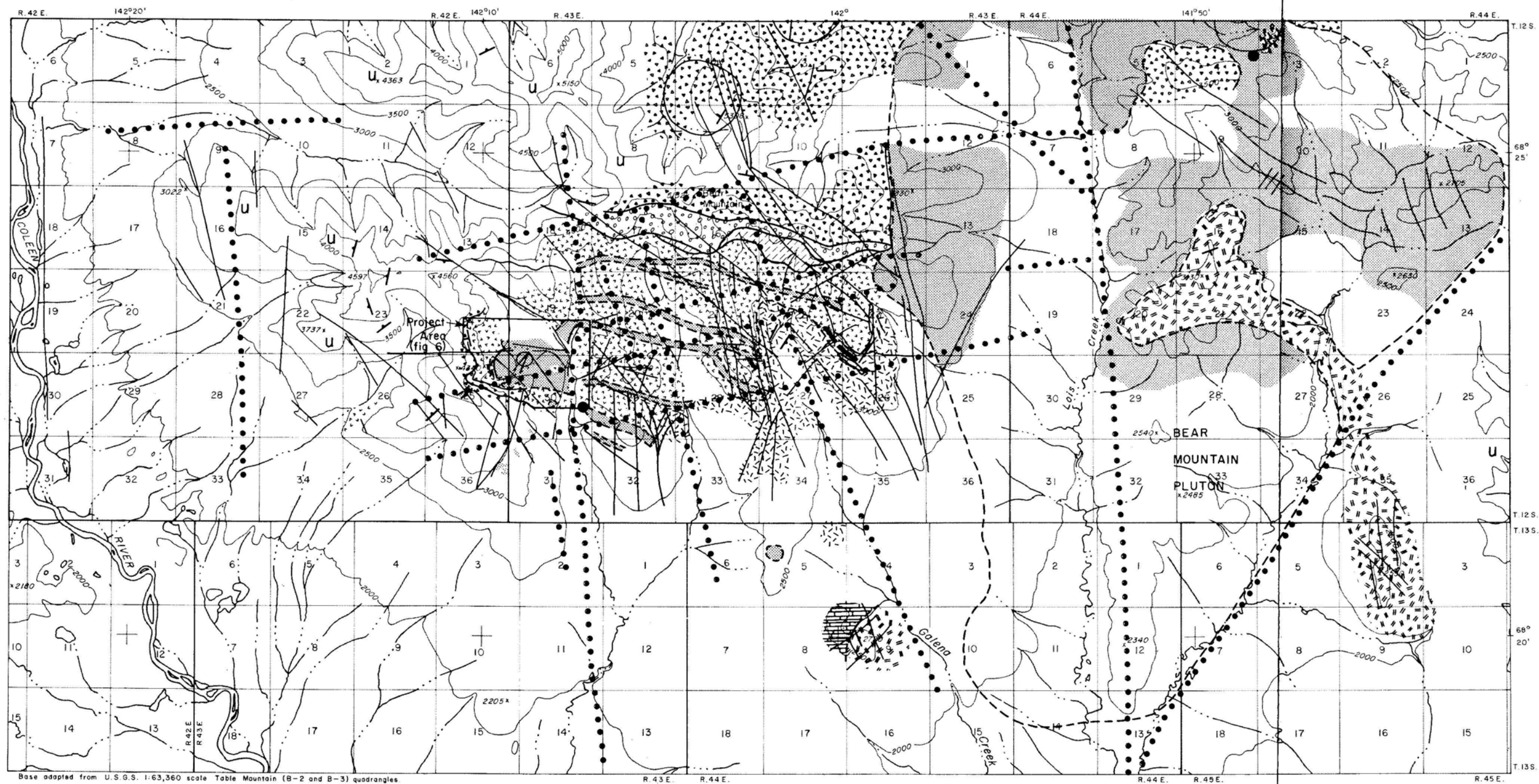


Figure 1. Index map of northern Alaska showing location of report area.



Base adapted from U.S.G.S. 1:63,360 scale Table Mountain (B-2 and B-3) quadrangles.

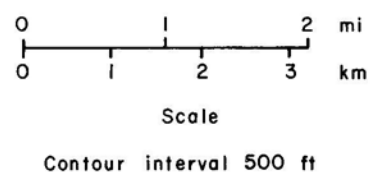


Figure 2. Regional geology of the Bear Mountain area.

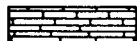
LEGEND

STRATIFIED ROCKS

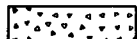
Mississippian - Devonian



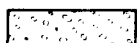
Lisburne Group - limestone.



Kayak shale.



Kekiktuk(?) - quartz-pebble conglomerate, includes grit and sandstone.

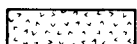


Kanayut - ferruginous conglomerate.

U

Undivided conglomerate is predominant rock type in area of symbol.

Devonian and Older

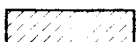


Siltstone and fine-grain sandstone, grading to phyllite.



Quartzite.

INTRUSIVE ROCKS



Greenstone - sills within the Devonian and older rocks.



Felsic intrusions - granite, rhyolite porphyry, and latite porphyry.



Mineralized veins of Pb-Zn-Cu-Ag.



Lithologic contact, dashed where inferred.



Lineament observed on aerial photography.



Lineament observed on Landsat imagery.



Strike and dip of bedding.



Strike and dip of bedding from aerial photography.



Location of K-Ar age determination.

the tungsten and molybdenum anomalies.

During field investigations by the Bureau in 1977, the occurrence was found to contain a pipe-shaped core of intrusive breccia. The presence of highly anomalous values of molybdenum, lead, and tungsten in soil and rock samples was also confirmed at that time (2, 18). The presence of trace amounts of accessory niobium (columbium)⁴ at Bear Mountain was also indicated (18).

⁴Niobium was accepted as the official name for the element by the International Union of Pure and Applied Chemistry in 1950.

Porphyry deposits of the type suspected to occur at Bear Mountain often contain associated tin and fluorine, which in addition to tungsten, are materials considered to be of strategic and critical importance to the United States.

In 1983, the authors spent 10 days mapping geology and conducting geochemical and geophysical surveys within a 1.5 mi² portion of the Bear Mountain area. The examination was limited to surface methods, and no drilling or excavation was attempted. This report describes the Bear Mountain porphyry occurrence and presents analytical and geophysical data.

The work upon which this report is based was done jointly under a contract agreement (contract no. P 4630243) between the Bureau of Mines and Dr. R. C. Swainbank, a geological consultant.

*** ACKNOWLEDGMENTS

The invaluable assistance of W. P. Brosge', geologist with the USGS, is gratefully recognized. In the 1960's, Brosge' collected the first geochemical samples indicating the presence of tungsten-molybdenum-lead

mineralization (7), and in 1976 he accompanied the first Bureau mineral investigation of the Bear Mountain area. His thoughts and critiques have contributed substantially to the present report. The assistance of Dr. M. Wiltse and N. Veach of the Alaska Division of Geological and Geophysical Surveys (ADGGS), who provided X-ray diffraction (XRD) determinations, is appreciated. Microprobe mineral identifications were done by J. Sjoberg, analyst, of the Bureau's Reno (NV) Research Center. The XRD determinations were performed by W. Barry, analyst, also of the Reno Research Center.

*** PROCEDURE

Sampling, geological mapping, and geophysical measurements were coordinated on a reconnaissance survey grid (fig. 3). The grid was constructed with 50-ft centers on lines 200-ft apart and is approximately 3,800 by 5,200 ft. A hip chain and compass were used and slope corrections were approximated. The east-west and north-south base lines of the grid intersect on a prominent iron-stained knob, referred to as the base station knob, in the west-central part of the grid. Approximately 70,000 linear ft of survey was completed, and about 1,300 stations were occupied.

Surficial weathering and alteration with prominent leaching mask bedrock with accumulations of clayey, iron-rich soils. Only about 1 pct of the map area is bedrock; therefore, bedrock lithologies were inferred almost entirely from frost-riven rock rubble. Due to the thick clayey soil accumulation, numerous frost boils (congeliturbates) are present. Because soil and rock chips from frost boils are naturally derived from depths of 3 ft or more, these features provide good sites for soil sampling and examining subsurface material. Soil samples were collected at depths of 6- to 8-in in frost boils or in residual mineral soil. Soil samples

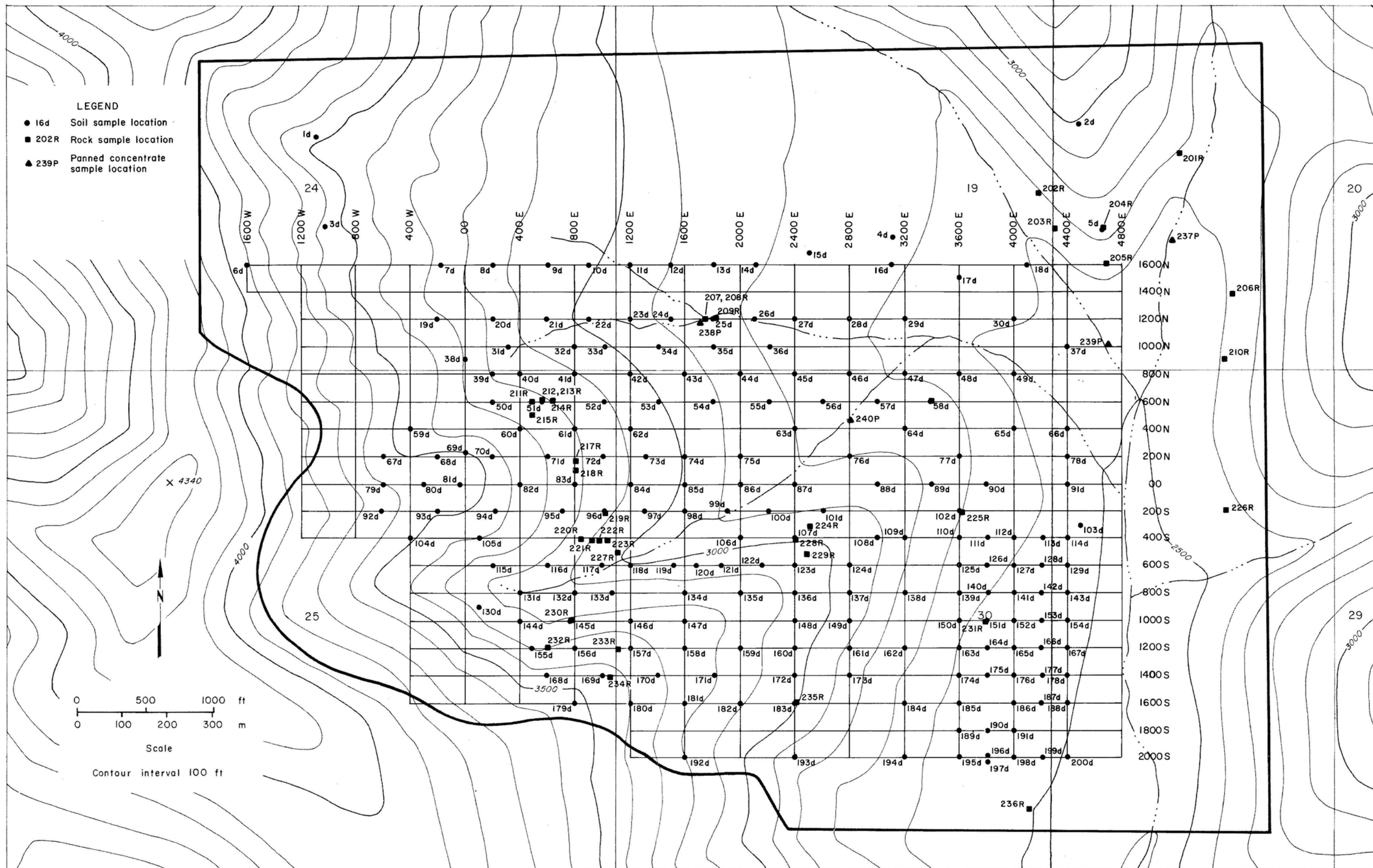


Figure 3. Survey grid and sample location map

were dried and screened at minus 80 mesh and the undersized fraction was pulverized.

Various rock samples were collected for elemental analyses, and petrographic, microprobe, and XRD mineralogical studies. Rock samples collected for analyses comprise a series of random chips from within several feet of a sample station. Samples were dried, crushed, and pulverized for analyses.

Heavy mineral concentrates were reduced from alluvial gravel collected with a steel shovel from the center of the stream beds. Volume of each gravel sample was measured on a loose basis. To compensate for the normal swell of excavated gravel, the in situ volume was calculated using a 25 pct swell factor. The bulk gravel sample was sieved to minus 0.25-in and further reduced by panning. The weight of the recovered concentrate was recorded followed by splitting for mineralogical microprobe study⁵

⁵Mineral composition was determined by microprobe studies by J. Sjöberg, of the Bureau's Reno (NV) Research Center Metallurgical Research Laboratory, and X-ray fluorescence analyses.

Analytical procedures used and the applicable detection limits are indicated in table 1. Analytical results and descriptions of soil samples are listed in appendix A; rocks with analyses are described in appendix B. All analyses were performed by the Bureau's Reno (NV) Research Center.

TABLE 1. - Quantitative analytical procedures and detection limits

Sample type	Element	Analytical procedure	Detection limit, ppm
Soil and rock.....	Ag	ICP ¹	0.7
	Au	...do.....	0.7
	Mo	ICP.....	1
	Nb	ICP.....	2
	Pb	ICP.....	30
	Sn	Atomic absorption..	5
	W	Colorimetric.....	5
Rock.....	Cu	ICP.....	5
	F	Chemical assay.....	10
	Li	...do.....	10
	Rb	...do.....	10
	Ta	X-ray fluorescence..	50
	Zn	ICP.....	2
	Panned concentrate...	Nb	X-ray fluorescence..
Sn		...do.....	100
Ta		...do.....	100
W		...do.....	100

ICP Inductively coupled plasma procedure.

¹ assay ton samples concentrated by fire assay prior to ICP.

Aerial photographs and images were evaluated to aid geological interpretation. Low-level, black and white oblique photographs of the project area included frames 10-93R to 10-97R taken in July of 1955. High altitude, false-color photographs were also reviewed and included frames 2520 to 2524 of line 36 taken in 1978. The Landsat image reviewed was frame 74-12 taken in September, 1977.⁶ Color photographs were

⁶Landsat and false-color photographs are on file with the Geophysical Institute, Photographic Library, 501 Elvey Building, University of Alaska, Fairbanks, AK. Black and white photographs can also be obtained through this library.

taken by the authors from an altitude of about 7,000 ft for more detailed geologic and structural interpretation.

Radiometric measurements were made with a single channel, gamma-ray scintillometer.^{8,9} Total-count readings were recorded at ground level on

⁸Mount Sopris Model SC-132 scintillation counter, Mount Sopris Instrument Co., Delta, CO.

⁹Reference to specific products does not imply endorsement by the Bureau of Mines.

50-ft stations along the east-west grid lines. The recorded data (appendix C) are the average result of at least two separate readings at each station.

In-phase and quadrature components of the earth's electromagnetic field were measured with a very low frequency electromagnetic (VLF-EM) receiver.¹⁰

¹⁰Geonics Ltd, Unit 8, EM-16, Mississauga, Ontario, Canada, L5Y1C5.

The Hawaii base station (NPM, frequency 23.4 KHz) was utilized because its signal direction deviates only 9° W from the north-south grid lines. All VLF-EM readings were taken on 50-ft stations while facing west, which was designated as the direction of positive dip angle, and the data (appendix C) were contoured according to procedures described by Fraser, 1969 (15).

Severe magnetic disturbances ranging from 100 to 3,000 gamma variations occurred throughout the period of the project and precluded magnetic measurements.

*** REGIONAL GEOLOGY

Quartzite of probable Lower Paleozoic to Precambrian age, Lower Paleozoic quartz-mica schist, and overlying Paleozoic phyllite, chert, greenstone, and quartzite (fig. 2), have been exposed in the middle to upper Coleen River Valley by a large domal uplift of post-Paleozoic age (11). Bear Mountain is located near the center of the uplift. Correlation of these rocks with those of other areas of Alaska is uncertain, but, like basement rocks of the Brooks Range they are part of the pre-Late Devonian foldbelt. The rocks may be more highly metamorphosed equivalents of similar rocks belonging to the Neruokpuk Formation of the Romanzof Mountains area to the north as described by Brosge' and others (6), Reed (17), Dutro and others (14), and Sable (19).

The Lower Paleozoic or older metamorphic units exposed near Bear Mountain are overlain unconformably by progressively younger Devonian to Mississippian Kanayut and Kekiktuk (?) conglomerates, Kayak Shale, and siltstone and limestone of the Lisburne Group (11). Northeastward Mesozoic or younger thrusting has resulted in structural complexity.

Granitic rocks have intruded the uplift at Bear Mountain to form the Bear Mountain pluton, a smaller stock, and numerous felsic dikes. Granite and biotite-quartz monzonite of the pluton are typically medium- to coarse-grained and locally porphyritic with large phenocrysts of potassium feldspar. Coarse equigranular syenitic variants are also present. Rhyolite porphyry occurs as phases within the pluton and also as a separate smaller stock which is the subject of this report. Rhyolite porphyry dikes cut the Paleozoic metamorphic rocks, as well as the pluton and the smaller stock. An interpretation of 1:1,000,000 scale aeromagnetic data in the vicinity of Bear Mountain suggests that the subsurface extent of felsic igneous rocks includes both the surface exposures of the Bear Mountain pluton as well as the stock and may continue in a narrow salient 20 miles further to the south (5).

The age of the Bear Mountain intrusion is tentatively Early Tertiary. Biotite from a syenite phase of the pluton yielded a potassium argon (K-Ar) age of 53.0 ± 1.6 m.y. Biotite from a rhyolite dike associated with the stock was dated at 56.4 ± 1.7 m.y. by K-Ar methods (4). Locations of age-dated samples are shown on figure 2. The granitic rocks have altered the Devonian and Mississippian rocks near the intrusive contacts to hornfels. Furthermore, the discordant northerly trend of the observed and interpreted outline of the pluton within the Devonian-Mississippian rocks and the lack of any thrust features within the granite

suggest emplacement after the regional thrusting of the Mississippian rocks.

Bear Mountain lies near the intercept of prominent north- and east-trending systems of topographic linears.¹¹ A major high-angle fault, inferred

¹¹This term is used to include all straight, curve, or circular features discernible on aerial photographs and satellite images.

by Brosge' and Reiser (8) to strike northeasterly from the Porcupine River area to the Canadian border near latitude 68° 15', forms the south-east boundary of the Lower Paleozoic or older basement rocks into which the Bear Mountain pluton has intruded. Landsat (satellite) imagery suggests that one or more northward splays of this fault extend toward Bear Mountain and correlate with north-trending linears which parallel both Lois and Galena Creeks (fig. 2). A second system of east-striking linears trends across the area of figure 2 from the Coleen River to Lois Creek. These linears coincide with a regional trend of domes and doubly-plunging anticlines in the pre-Mississippian basement which extends eastward from Table Mountain to Ammerman Mountain and beyond into Canada (4).

*** LOCAL GEOLOGY

SURFICIAL GEOLOGY

The map area (fig. 3) and vicinity is characterized by subdued, tundra- and rubble-covered, rounded hills with maximum local relief of approximately 2,500 ft. Cirque and valley glaciation has occurred in the uppermost valleys to the north of the map area, however, the extent of local glaciation has been obscured by weathering and erosion.

Extensive weathering and colluvium caused by frost riving and chemical leaching has masked altiplanation terraces, common features elsewhere in the Brooks Range. The relatively thick clayey soil and colluvium on the

lower and intermediate slopes exhibit abundant solifluction lobes and frost boils. Rock rivering frequently occurs on the higher slopes. Because the latitude of the area is higher than 68° N, continuous permafrost should be expected.

Actively downcutting streams above the 2,500-ft elevation have formed a topographic bowl-like depression approximately 2,000 ft in diameter in the north central portion of the map area. A prominent bench on the southeastern slope of the bowl lies approximately 100 ft above the present stream bed, indicating fairly recent and substantial downcutting (fig. 4). Below the 2,500 ft elevation, the drainages combine into a single meandering channel with low alluvial benches. The width of the active and terrace alluvium below 2,500 ft is estimated to range from about 400 to 1,000 ft immediately below the bowl to slightly less further downstream.

LITHOLOGY

Metasedimentary and igneous rock types are present in the map area, however, contact relationships between units are obscured by abundant rubble on hillsides. Metasedimentary rocks consist of a siltstone-phyllite unit and a quartz-pebble conglomerate unit (fig. 5). Intrusive rocks include quartz porphyry, rhyolite porphyry, and intrusive breccia. Intensive surficial and hydrothermal alteration of the porphyritic igneous rocks frequently hinders petrographic classification.

Metasedimentary Rocks

The oldest unit mapped consists of fine-grained, green to dark gray siltstone and phyllite (Pzp) with a minor silty limestone component. The green coloration is more common in the phyllite and probably caused by chlorite and locally epidote metamorphic minerals. Estimated thickness of the Pzp unit west of Galena Creek is about 1,500 ft, although structural



FIGURE 4. - Photograph looking southeast showing the surficial geology. The topographic bowl-like depression lies to the left of the photo. Note the prominent bench to the right of the creek in the upper left of the photo. The base station knob is located in the lower center area.

LEGEND

Metasedimentary Rocks

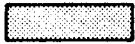


Quartz-pebble conglomerate and sandstone.

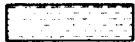


Siltstone and phyllite.

Intrusive Rocks



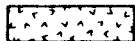
Rhyolite porphyry and aplite dikes.



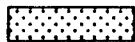
Breccia - a) intrusive breccia containing rounded to subrounded clasts of quartz porphyry, rhyolite, and rhyolite porphyry, and subangular to angular clasts of quartz porphyry, hematized siltstone, and quartzite in a clastic matrix of similar composition; b) intrusion breccia containing rounded to angular clasts in an aphanitic groundmass.



Rhyolite porphyry with phenocrysts of K-feldspar and doubly terminated quartz. Frequently contains visible fluorophlogopite. Rhyolite porphyry dikes may be related to this phase. Dot pattern where Rp rubble indicates dikes exist.



Altered rhyolite porphyry with quartz phenocrysts and extensive alteration of K-feldspar.



Silica-rich rock and quartz porphyry, may include areas of highly silicified metasedimentary rocks. A sugary silica (saccharoidal) groundmass is typical, grading to hard chalcidonic matrix in the most intensely silicified zones.



Undivided rhyolite porphyry, quartz porphyry, quartz latite, gossan and silica-rich rock.

Alteration



Continuous to semi-continuous limonite-goethite-hematite-jarosite gossan, and/or iron-rich clay. (X) - location of gossan of unknown or limited extent.



Pyritization or intense iron-oxide staining.

Q

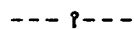
Quartz veining.

A

Intense argillic alteration.

M

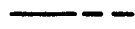
Muscovite.



Contact approximated from aerial photography.



Contact, dashed where inferred.



Fault, dashed where inferred.



Approximate trace of prominent linear feature from Landsat imagery.



Approximate trace of linear feature from aerial photography and observations.



Dip and strike of bedding.



Dip and strike of prominent jointing.



K-Ar age determination.

Note.--Rock types are divided where a single rubble type predominates, outcrop occurs in less than 1% of the map area.

repetition is possible (18). Minor greenstone rubble was found among predominant Pzp talus indicating sills or dikes are present. The unit is exposed on most of the perimeter of the stock (fig. 5) and an intrusive contact relationship is evident on the basis of thermal effects such as bleaching, baking, and development of hornfels and tactite.

Quartz-pebble conglomerate (Mcg) crops out along higher ridges on the west and southwest edge of the map area and overlies the Pzp unit (fig. 5). The conglomerate weathers to a gray-white color and is predominantly composed of 0.25- to 0.5-in pebbles of clear to milky white, subrounded quartz and lesser chert in a silicified sandy matrix. Locally, pebbles are coated with clay. Barren, white, randomly oriented, quartz veinlets also commonly cut the conglomerate. Blocks of light-colored grit and quartzite, which are mixed with the conglomerate rubble in the southern part of the map area, are probably derived from intercalated beds within the conglomerate unit. The thickness of the unit is unknown, but near Bear Mountain immediately north of the map area, it may be several thousand feet (18).

At their contact, the Mcg and the porphyritic rocks appear to be highly silicified. The contact is best viewed on the east side of the base station knob (grid station 00N, 00E - fig. 3) where, proceeding downhill, pebbles become progressively less distinct from the conglomerate matrix, although rounded quartz pebbles can still be seen on the weathered surface. Further downhill, highly silicified porphyritic rocks can be identified. The massive silica rubble found on the ridge between 300 to 2,500 ft west of the eastern creek junction also exhibits similar evidence of a silicified contact zone with the conglomerate.

Intrusive Rocks

A complex of porphyritic igneous rocks is exposed in rubble for approximately 2,500 ft in a north-northeasterly direction for at least 4,500 ft in an east-southeasterly direction (fig. 5). The relationship between the main intrusive complex and an isolated small body of intrusive rock in the extreme northeast corner of the map area is uncertain, as is the relationship of this complex to the nearby Bear Mountain pluton (fig. 2). Four phases of intrusive rock were recognized in the map area: quartz porphyry, rhyolite porphyry, intrusive breccia, and rhyolite porphyry and aplite dikes.

1. Quartz porphyry (Qp) typically has a sugary, quartz-rich groundmass, with minor amounts of muscovite and potassic feldspar and phenocrysts of quartz which occur as clear, bipyramidal or rounded grains. Topaz, a common accessory mineral in this phase was found by X-ray diffraction (XRD) analyses to be locally a major component of this rock. Finely disseminated accessory opaque minerals including wolframite (identified by XRD analyses) are pervasive. The Qp distinguished by the predominance of quartz over potassic feldspar phenocrysts and groundmass feldspar, generally occurs at higher elevations and along the outer edges of the complex. Near the intrusive contact, undifferentiated areas of highly silicified metasedimentary rock may also be included.

2. Rhyolite porphyry (Rp) is the most abundant phase of the intrusive complex. The Rp contains clear, bipyramidal quartz and potassic feldspar phenocrysts in a fine-grained groundmass consisting of approximately equal amounts of potassic feldspar and quartz. Simple Carlsbad twinning was observed in some of the abundant feldspar phenocrysts, but petrographic examination showed that most of the groundmass feldspar was altered to

very fine-grained phyllosilicate and clay minerals. Muscovite and kaolinite were identified by XRD analyses (see sample descriptions in appendix B). Locally, the phyllosilicates are purple, or less commonly, green. Microprobe examination indicated the coloration is likely due to manganese. The central portions of the feldspar phenocrysts are also altered, whereas the rims are generally less altered. A crosshatch preferred orientation of much of the muscovite in some of the rhyolite porphyry suggests alteration of microcline. In figure 5, rhyolite porphyry is subdivided on the basis of the degree of alteration, where (Rp) indicates rock with relatively unaltered feldspar phenocrysts, whereas (Rpa) denotes pervasive alteration and feldspar destruction. Further distinction of the Rpa on the basis of geochemical and geophysical data will be discussed later.

3. Intrusive breccia¹² (Rb) occurs in the west-central area of the

¹²The definition of intrusive breccia and the clear distinction between intrusive and intrusion breccia is as discussed by Bryant (12).

complex. The actual extent of the Rb is inferred due to cover by colluvium and gossan. The breccia (fig. 6) consists of rounded to subrounded clasts of quartz porphyry, rhyolite, and rhyolite porphyry, subangular to angular clasts of quartz porphyry, siltstone, and quartzite, and a matrix composed of finely comminuted material derived from the same rock types. The rhyolite and rhyolite porphyry clasts are argillically altered (kaolinite identified by XRD analyses) and small patches of extremely fine-grained black silica occur in the matrix and as clasts (verified by XRD analyses). Several hundred feet to the north of the southern stream (fig. 5) a breccia of rhyolite and rhyolite porphyry fragments occurs in a groundmass of muscovite, quartz, and iron and manganese oxides.



FIGURE 6. - Intrusive breccia near station 1000E - 600S.

4. Rhyolite porphyry and aplite dikes (Rd) cut both the intrusive complex and the metasedimentary rocks and form local topographic highs. The dikes are composed of bipyramidal, smokey-colored quartz and potassic feldspar phenocrysts in a fine-grained groundmass consisting of nearly equal amounts of quartz and feldspar with minor amounts of biotite. Accessory pyrite locally occurs in these rocks.

STRUCTURE

Structure of the map area is characterized by a dome-like uplift associated with the intrusive complex. The uplift is located at, and apparently controlled by the intercept of prominent linear features and faults.

A domal structure similar to that seen regionally is evident in the vicinity of figure 5. Limited bedrock measurements and aerial photographic observations on the west side of the intrusive complex indicate the sedimentary rocks dip westward, away from the intrusion. On the basis of high-altitude aerial photographs an outward dip is also suspected to the southwest of the complex. The conglomerate unit just north of the map area has been previously reported (18) to dip northward (fig. 2).

The two prevailing regional systems of linears previously described (fig. 2) are present in the map area. A linear from each system transects the map area (fig. 5). The east-trending linear aligns approximately with the upper creek valley south of the base station knob and correlates with the portion of an interpreted fault contact between the Rpa and a pendant (?) of Pzp. On the ridge further eastward it is marked by topographic depressions. The second linear follows the north-trending valley in the east part of the map area and is spatially coincident with the eastern perimeter of the intrusive complex.

A circular topographic high underlain by Rp located in the central part of the map area is visible in the left central area of figure 4. Three linear topographic features intersect within the circular feature.

Inferred faults shown on figure 5 appear to have displaced lithologic units. Faults are indicated by two subparallel northeast-trending linear features that correspond in part to portions of the stream channels on either side of the base station knob. Both trend more westerly at their southwest extremities. In the central part of the intrusive complex two east-southeast-trending zones of gossan contain slickensided rubble. Both of these zones follow the trend of the principal gossan zone (shown in fig. 5) and are inferred to be fault zones. In the northeast part of the map area, rubble of massive silica and abundant vein quartz occurs along the northwest-trending linear paralleling the creek bed. The linear forms the prominent southwest margin of the isolated body of intrusive rock and suggests a zone of faulting.

AGE RELATIONSHIPS

The siltstone-phyllite unit in the map area (Pzp) is inferred to be Upper Devonian on the basis of fossil evidence. Fossil plant fragments of unbranched axial stems were found in the Pzp unit 1,200 ft north-northeasterly of the base knob, at an elevation of 3,150 ft. An examination by S. H. Mamay of the USGS was indeterminate and could only indicate a Mississippian or earlier age (4). A second collection of similar fossils made by J. Dillon (13), however, provided a probable Upper Devonian age. The Pzp unit is further indicated as pre-Late Devonian on the basis of its structural relationship with the overlying quartz-pebble conglomerate (Mcg).

Conglomerates of the eastern Brooks Range are believed to have formed during outpourings of sediment during a Late Devonian to Mississippian orogeny (6, 19). They overlie the Paleozoic or older basement with an angular unconformity. The light-colored, quartz-pebble conglomerate with a siliceous matrix (Mcg) probably correlates to the Mississippian Kekiktuk Conglomerate described by Brosge' (6, 11), Sable (19), and other investigators in the region.

The felsic, multi-phased complex clearly intruded and thermally altered both the Pzp and Mcg at a relatively high level of emplacement. Age relationship of the complex to the nearby Bear Mountain pluton is uncertain.

Rhyolite and aplite dikes are common in the map area, as well as in the general Bear Mountain vicinity where they have been observed to cut the other Paleozoic lithologies. Dikes appear to cut the Qp and Rp rocks in the southern portion of the map area and to form a southeast- to east-trending swarm cutting the Pzp unit. This trend can be traced eastward out of the map area, across Galena Creek toward the Bear Mountain pluton (fig. 2). Near Lois Creek, dikes also intrude coarse-grained syenite and granite. Location of the previously mentioned K-Ar dated rhyolite porphyry dike (56.4 ± 1.7 m.y.) is shown in figure 5.

ALTERATION

Several types of alteration were recognized, some of which were not restricted to individual rock units. These include

- 1) iron oxidation
- 2) pyritization
- 3) propylitic alteration
- 4) argillic alteration

- 5) sericitic alteration
- 6) silicification.

Iron Oxidation

A gossan zone shown on figures 5 and 7 is the most striking alteration feature of the map area. Pervasive oxidation of, presumably, pyrite to hematite, limonite, goethite, and other oxides is discussed in greater detail in a later section on mineralization. Jarosite is often associated with the intensely oxidized rocks. In the extreme northwest of the map area the Mcg is intensely altered to a matrix of clay, limonite, gossan, and mica and is on strike with the principal gossan zone.

Moderate iron oxide staining is present in both the metasedimentary and igneous rocks and has resulted in pervasive brown weathering surfaces (fig. 7). Intense hematitic staining is restricted to the western periphery of the complex above the base station knob.

Pyritization

Disseminated relict pyrite crystals occur in altered Rp near the southwest margin of the intrusive complex (samples 230R and 233R, fig. 3). Pyrite also occurs in the hornfels formed in Pzp on the eastern end of the intrusive complex.

Propylitic Alteration

Propylitic alteration, comprising chlorite, epidote, and calcite, is particularly noticeable in the metasedimentary rocks close to the intrusion in the east-central part of the map area. Muscovite and quartz veins are also commonly associated with these rocks.

Argillic Alteration

Kaolinite, generally associated with muscovite are minor constituents of the Rp-Rpa phase, and less commonly of the Qp phase (appendix B).

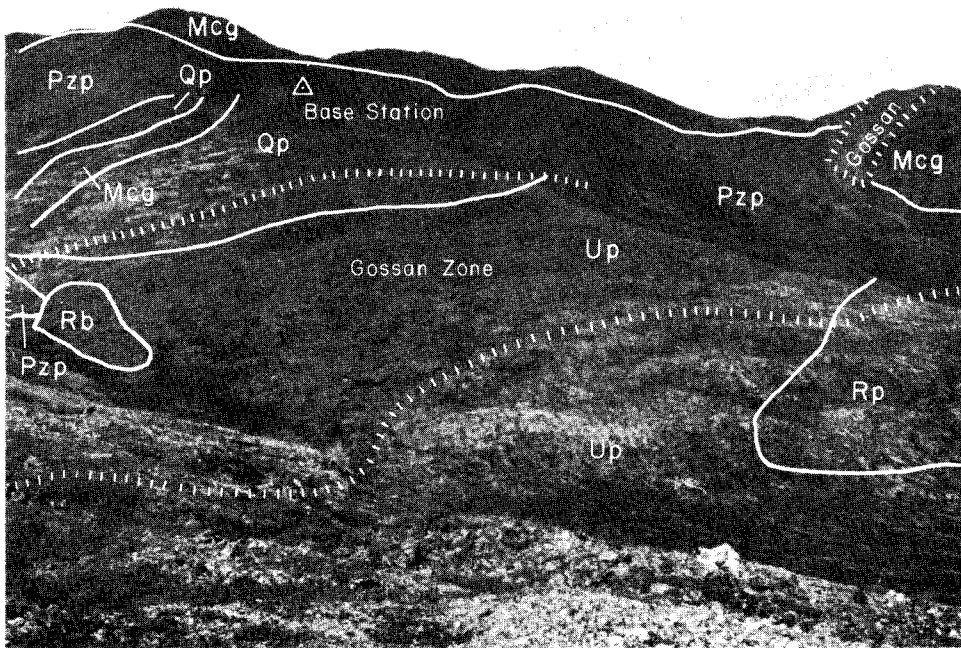


FIGURE 7. - Photograph showing alteration and intrusive phases of the subvolcanic complex. Photo was taken looking northwest from station 2400E - 400S. Note the red hematization on the western margin of the complex and the red-brown coloration associated with the northwestern end of the gossan zone. Light-colored solifluction lobes are a common feature.

EXPLANATION

Metasedimentary rocks:

- Mcg - quartz pebble conglomerate.
- Pzp - siltstone and phyllite.

Intrusive rocks:

- Rb - intrusive breccia.
- Rp - rhyolite porphyry.
- Qp - quartz porphyry with topaz and silica-rich rocks.
- Up - undivided porphyry and silica-rich rocks.

Groundmass feldspar is more strongly altered to clay than is the phenocryst feldspar.

Sericitic Alteration

Analyses by XRD indicate muscovite to be the only mica mineral detectable (appendix B). Muscovite (including probable sericite) occurs as very fine-grains and commonly is a minor to major component of the Rp and Rpa rocks. Groundmass potassic feldspar is commonly completely replaced by quartz, muscovite, and clay, whereas feldspar phenocrysts show a complete gradation from unaltered to pervasively altered varieties. This alteration grades from a) weakly argillized and sericitized phenocrysts to b) partially replaced crystals with discrete muscovite crystals in a central void surrounded by a thin irregular clay rim to c) totally replaced phenocrysts where only the shape and a few fragments remain to identify the former phenocryst (Rpa). The Rpa, which has a vuggy or scoriaceous appearance due to the surficial leaching or removal of feldspar, is most common in the southwestern part of the map area, particularly near and within a dike-like body extending to the southwest.

Locally, masses and disseminations of phyllosilicate (muscovite?), particularly in the Rp unit, have a distinctive purple color, particularly on moist rock surfaces. Examination by microprobe did not reveal the presence of lithium or fluorine and suggested that manganese is the cause of the coloration. Green variants are also present but less common.

Silicification

Progressive silicification occurs along the outer parts of the Qp phase of the complex. Width and degree of intensity of the zone of recognizable silicification appear to be highly variable. The degree of variation intensity is exemplified at grid station 1600E and 800S. Quartz porphyry

contains clear, bipyramidal quartz phenocrysts and less common altered feldspar phenocrysts in a sugary quartzose groundmass. Voids indicate the former presence of feldspar phenocrysts in some rocks. Rubble nearby is similar, but the matrix is altered to extremely fine-grained silica, often cut by veins of gray chalcedonic quartz. In some rubble the relict feldspar phenocrysts are also silicified, and even the voids are filled in by cryptocrystalline silica. In the most highly silicified rubble in this area even the crystal boundaries of the clear quartz phenocrysts are embayed by silicified groundmass. Local annealing of numerous fractures by several generations of randomly oriented quartz veins and veinlets has also occurred.

A dark gray blockfield of extremely silicified rock occurs on the east flank of the base station knob and is visible in figure 7. Much of this rubble contains open, limonite-coated fractures with some vein quartz infilling. Microscopic examination of this rock shows fragments of clear, rounded to subangular quartz that could be derived from either dismembered quartz pebbles or glomeroporphyritic quartz phenocrysts that have undergone partial resorption. Origin of the silica masses is uncertain. Near the top of the knob, the less altered original Mcg unit can be clearly distinguished.

Silicification is generally weak in the rhyolite porphyry (Rp) rubble and quartz is generally confined to veins only. Some of the massive slaggy gossan is silicified to the extent that the limonite resists scratching with a knife. Some jarosite (identified by XRD analyses) veins and fracture fillings in Qp are also silicified to the same degree.

Other Alteration

Mineral identifications by petrography and XRD indicate other alteration phases may be present. Small euhedral crystals of magnetite, possibly secondary, occur in both the Rp and Qp. Small skeletal magnetite crystals are also present in sample 207R. Garnet was identified in gossan sample 231R, but whether it is related to an alteration phase is also uncertain. Topaz was repeatedly identified and is particularly prevalent in Qp rocks (appendix B), indicating a fluorine-rich magma source. It could not be determined whether the topaz is primary or a secondary form of fluorine alteration.

*** GEOPHYSICS

The VLF-EM and radiometric surveys were conducted simultaneously, and details of the methods and instruments used are described in the procedure section of this report. The geophysical data are presented in appendix C.

RADIOMETRIC SURVEY

Radiometric readings, in total counts per second, were contoured in intervals of 50 cps, beginning with the highest values. The interpretative contours are shown in figure 8.

Areas where rhyolite porphyry rubble (Rp) predominates are characterized by readings in excess of 300 cps. The two main areas thus defined are separated by a northeast-trending linear zone of total counts less than 200 cps. This zone is in part coincident with surficial deposits along the creek draining the south side of the base station knob and also coincides with an inferred fault.

The northern limit of radiometric readings exceeding 150 cps is well

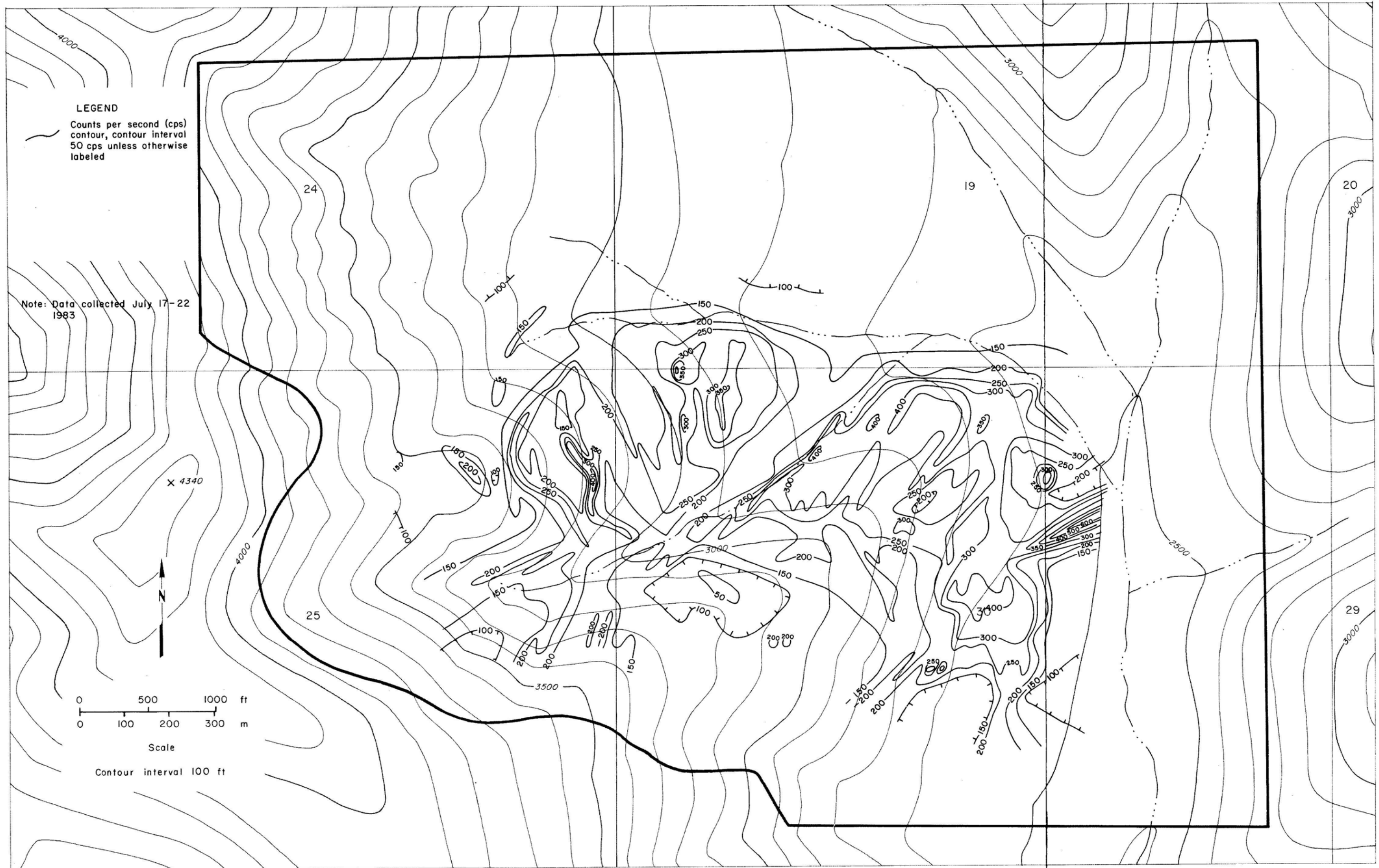


Figure 8. Interpretative contouring of total-count radiometric values in counts per second.

defined along the east-west margin of surficial cover, whereas the southern limit is disrupted by several linear zones associated with dikes (Rd) in the southwest and southeast quadrants of the grid. Several linear zones of elevated total cps radiate from the vicinity of grid location 600S-1200E and also from the grid location 1200S-3600E.

Radiometric readings are generally less than 150 cps in tundra-covered areas, especially if moist or wet, but an east-northeast zone of particularly high readings is associated with limonitic clayey-silt in frost boils in tundra near grid station 600S-4400E. Readings over isolated frost boils were greater than 1,100 cps. High total counts (>400 cps) were also obtained over gossan rubble at the 3,200-ft level on the east flank of the base station knob. Total count measurements associated with metasedimentary rocks and the Rpa phase in the south central part of the map area were particularly low.

VLF-EM SURVEY

Dip angle readings and measurements of quadrature components indicated that causative bodies are either flat-lying or weak conductors. The null-points were quite distinct, but the magnitudes of both the in-phase component, given by the dip-angle readings, and of the quadrature component, were generally small.

In-phase component

Dip angles were measured directly, and the values were filtered by methods described by Fraser (15). Because there was little variation in measurements, the filtered values are contoured in figure 9 at five unit intervals and include the zero value.

Examination of the contoured data indicates the strongest conductor to be a sinuous zone extending south to north across the base station knob.

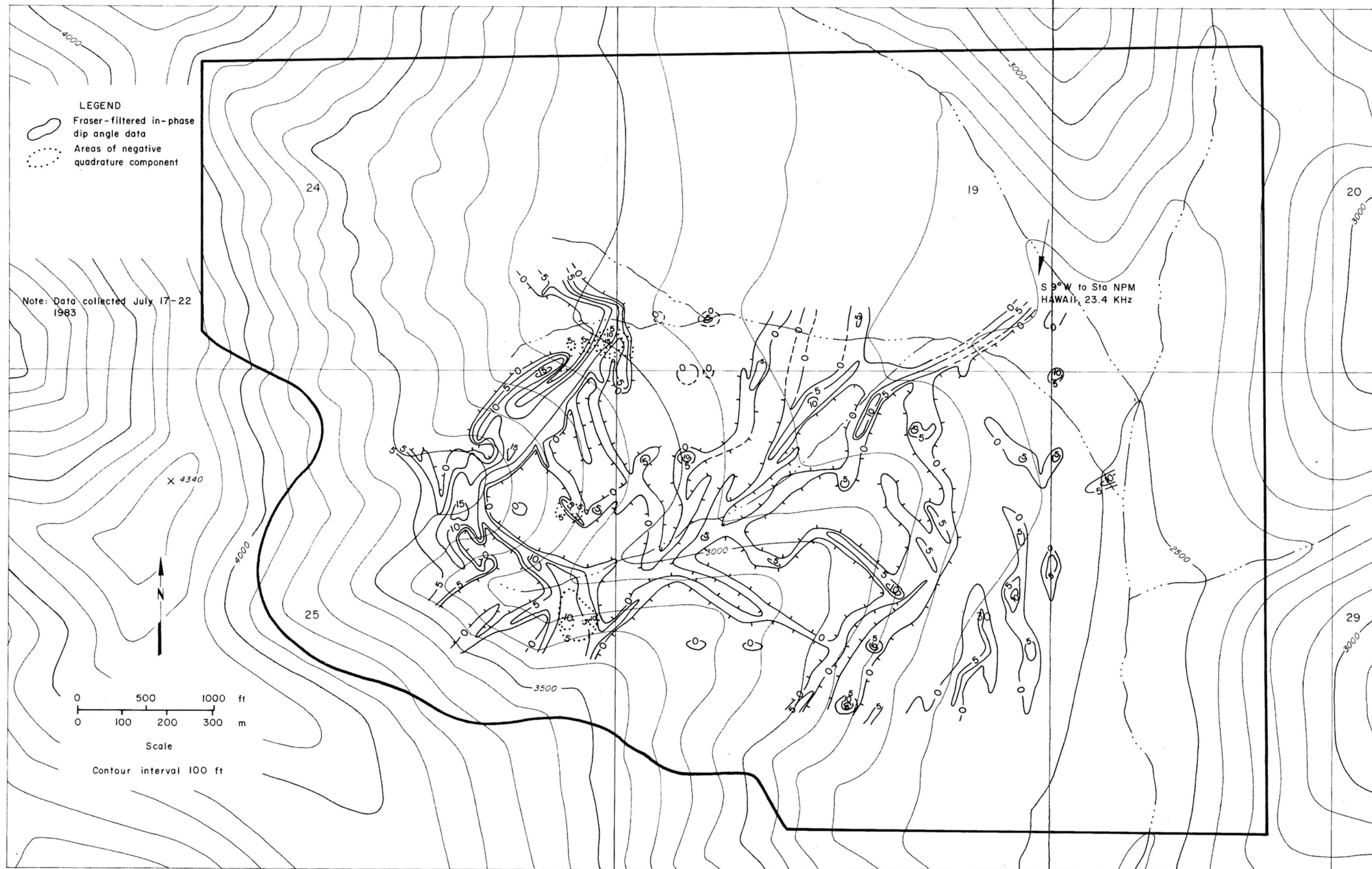


Figure 9. VLF-EM survey map.

This zone trends northwest at the north end, coincident with an area where the quadrature component is negative. A complex zone of weak to moderate conductors trends northeast across the map, coincident with an inferred fault and a zone of low radiometric total-count values. Several linear zones of weak conductivity at the southwestern end of this zone align with Rd rubble.

An area centered approximately on 600N-1800E grid station has no indication of conductive rock. This area coincides with the circular feature characterized by radiometric total counts in excess of 300 cps.

Quadrature Component

The quadrature component is generally weakly positive, indicating that the causative bodies are probably shallow. Moderately negative values of the quadrature component centered on grid stations 1000N-1000E and at 900S-800E have a very limited areal extent and may indicate more deeply buried conductive bodies.

*** GEOCHEMISTRY

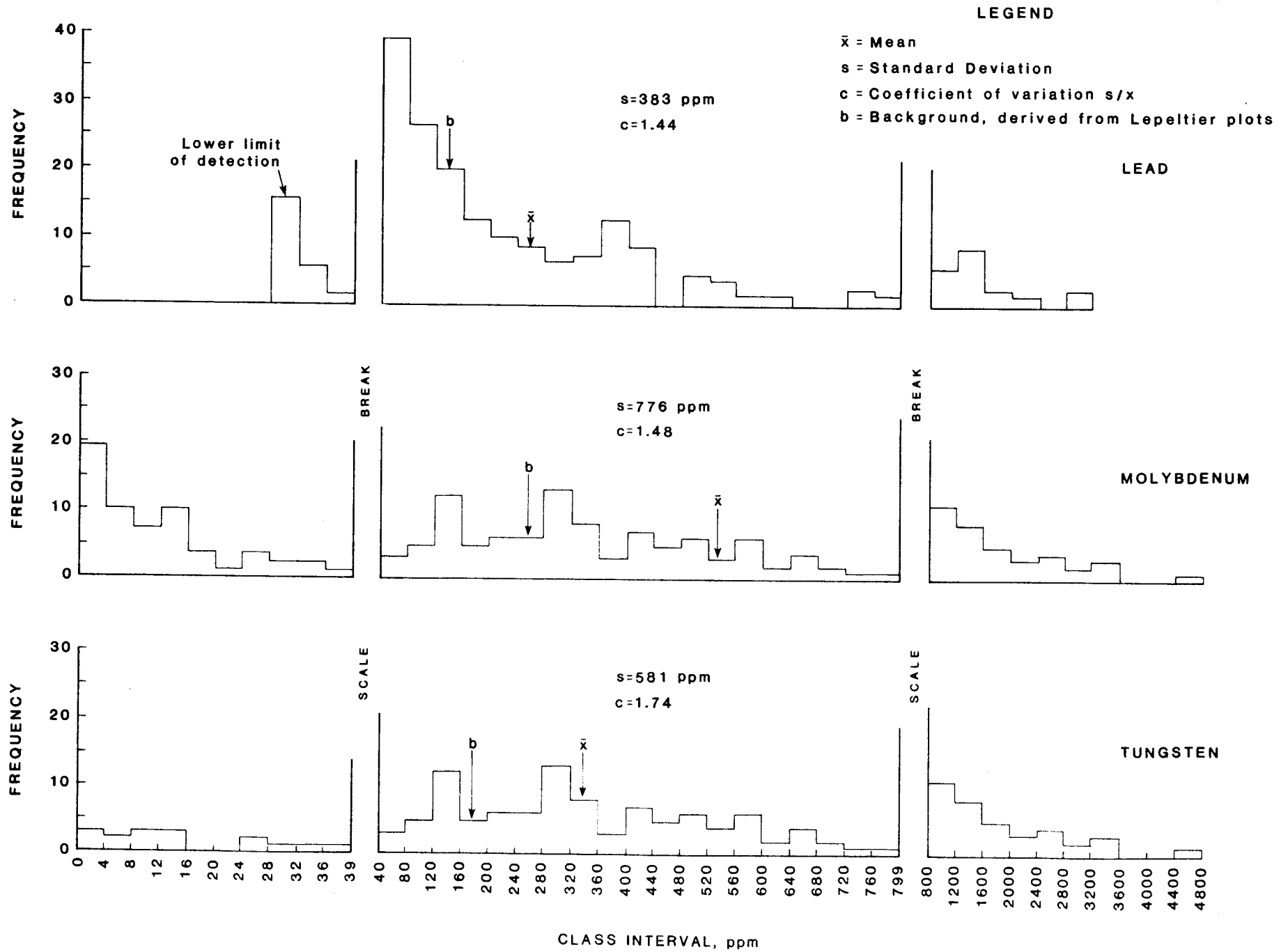
Analyses of 200 soil and 36 rock samples show that molybdenum, lead, and tungsten are present in abundance whereas niobium is present, but at less anomalous levels. Gold, copper, zinc, and silver were generally present in only very low amounts or not detected. Detectable values for tin were also found sporadically in soils and rocks. Soil sample 174d contained 162 ppm Sn. Also of note was 55 ppm Sn in soil sample 1d located in the northwest gossan area. Fluorine was present in some of the rock samples which were analyzed for that element. Samples containing topaz are associated with the higher fluorine values (up to 2.2 pct F in sample 212R) (see appendix B and fig. 3).

The soil sample population as a whole is largely confined to an area

underlain by mineralization that contains obviously anomalous amounts of lead, molybdenum, niobium, and tungsten when compared to the crustal abundance values given by Brooks (3). It was not possible to extend the sampling grid sufficiently far enough beyond the mineralized area so to determine local background levels of metals in soils overlying unmineralized rock. Some statistical parameters for the anomalous data sets of soil lead, molybdenum, and tungsten values are shown in figure 10, which presents frequency distribution histograms for the analytical data in appendix A. Because the mean metal values are skewed due to the influence of the mineralized system, the background values, standard deviations, and other statistical parameters for data reduction should be used with caution. Figures 11 through 14 show the contoured values of molybdenum, tungsten, lead, and niobium in soil.

Values of 600 ppm molybdenum and 500 ppm tungsten are commonly used in the literature to describe the content of molybdenum and tungsten in porphyry systems (16, 22-23). These values are approximately equivalent to 0.1 pct MoS_2 and 0.06 pct WO_3 . At the Climax Mine in Colorado, 0.1 pct MoS_2 is the assay plan minimal limit and higher grade parts of the "Upper Ore Body" tungsten zone average about 0.06 pct WO_3 (22). Because soil sampling at Bear Mountain was restricted to a mineralized system, these commonly accepted values for molybdenum and tungsten in porphyries were chosen arbitrarily as threshold levels for anomalous soil values. It should be noted that while anomalous soil values are a reflection of an anomalous metal content in nearby bedrock the two values are not necessarily coincident. Metal content in soil can often be somewhat depleted or concentrated depending on local ground water and chemical environments. Soil values of lead were arbitrarily selected for direct

Figure 10. Cumulative frequency histograms of soil metal values (lead, molybdenum, and tungsten).



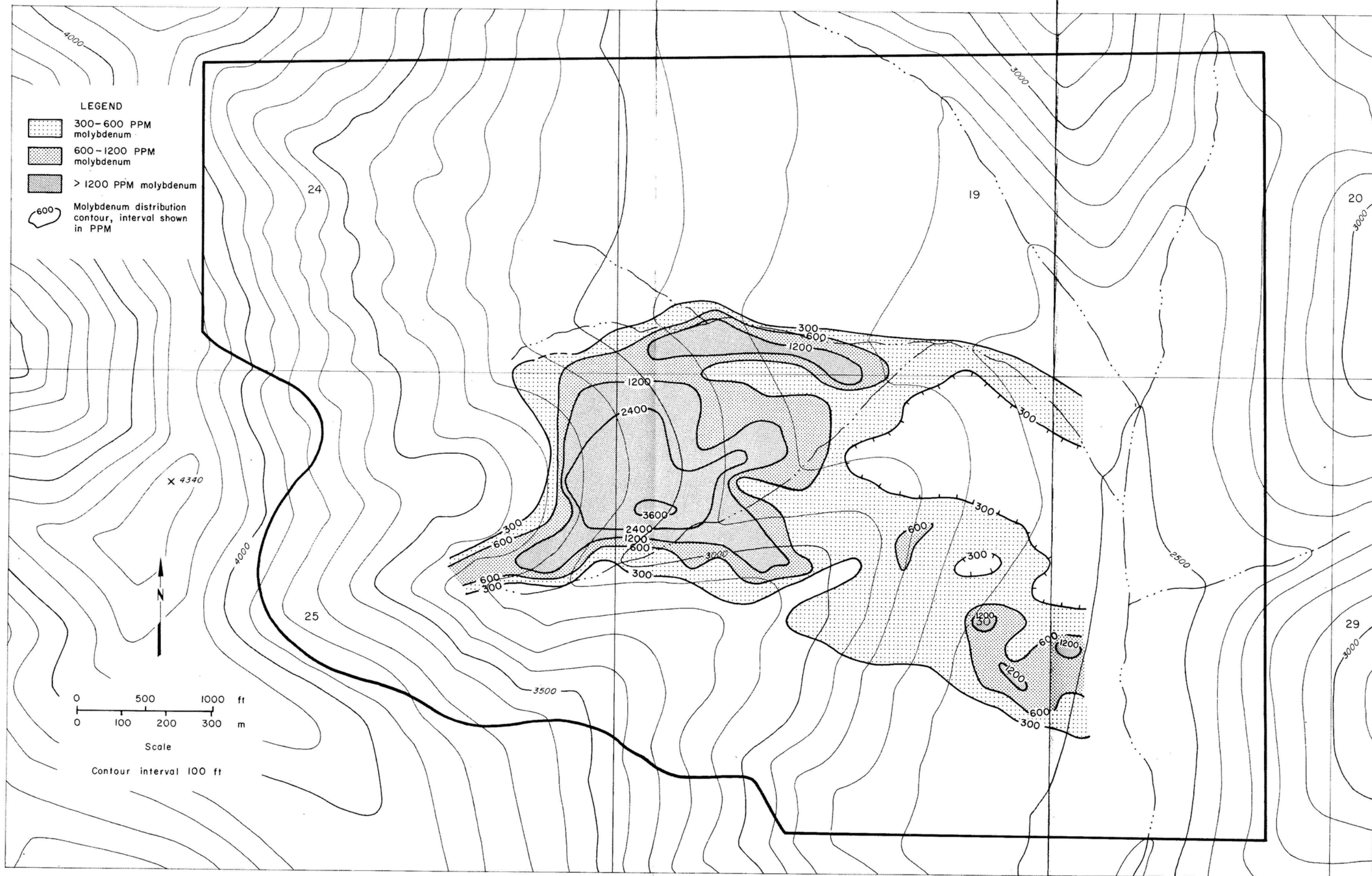


Figure 11. Distribution of molybdenum in soils.

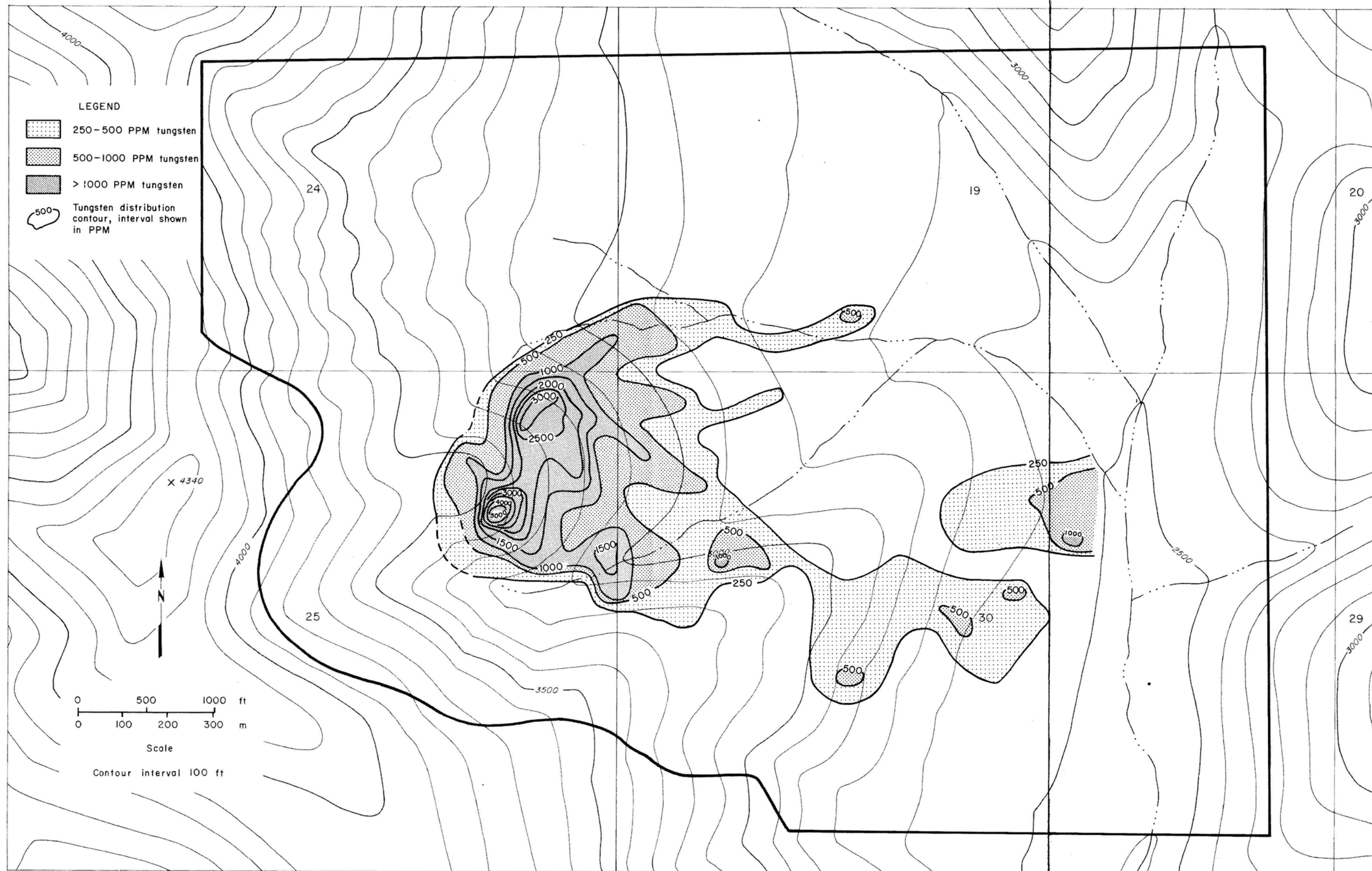


Figure 12. Distribution of tungsten in soils.

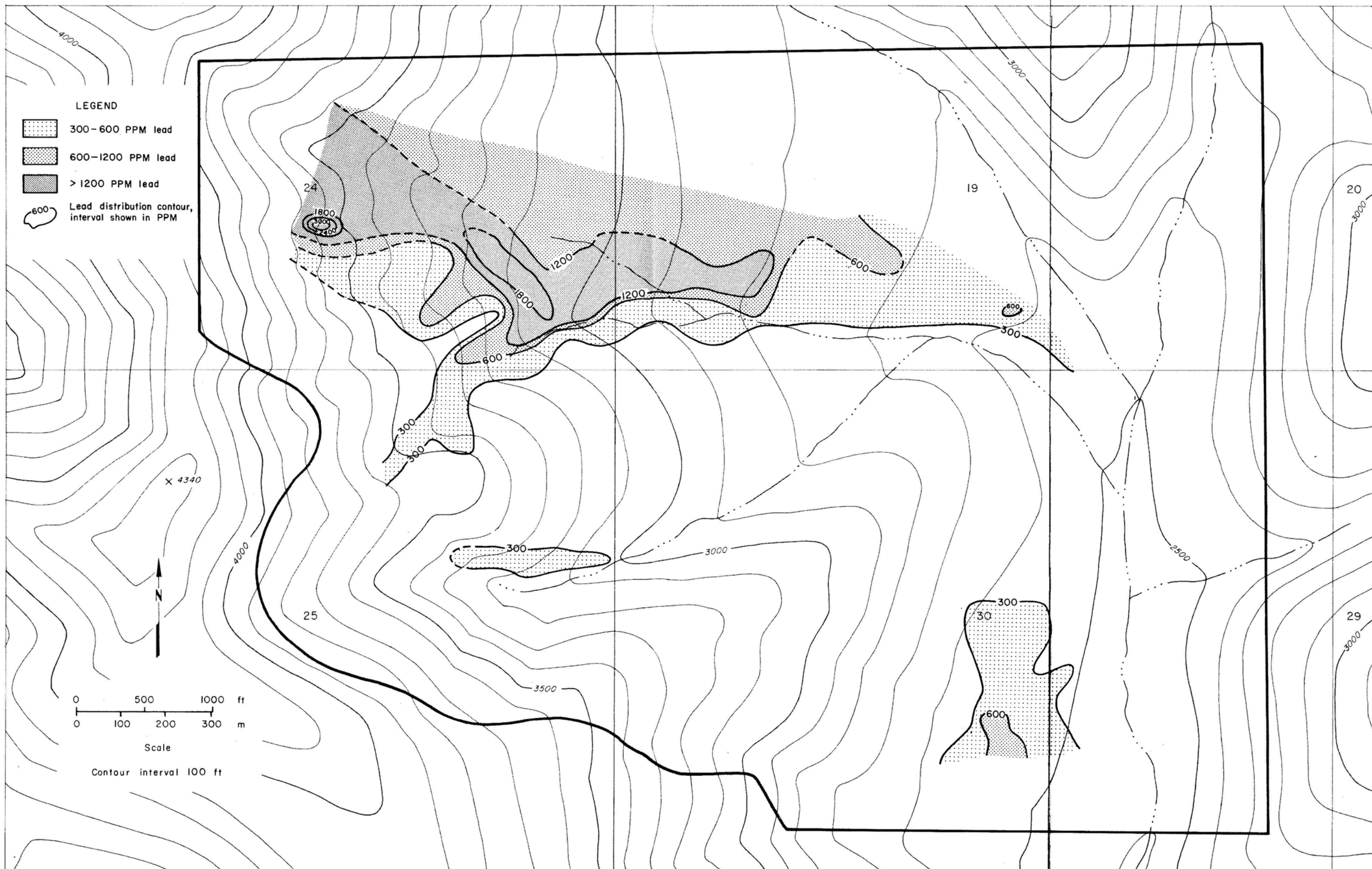


Figure 13. Distribution of lead in soils.

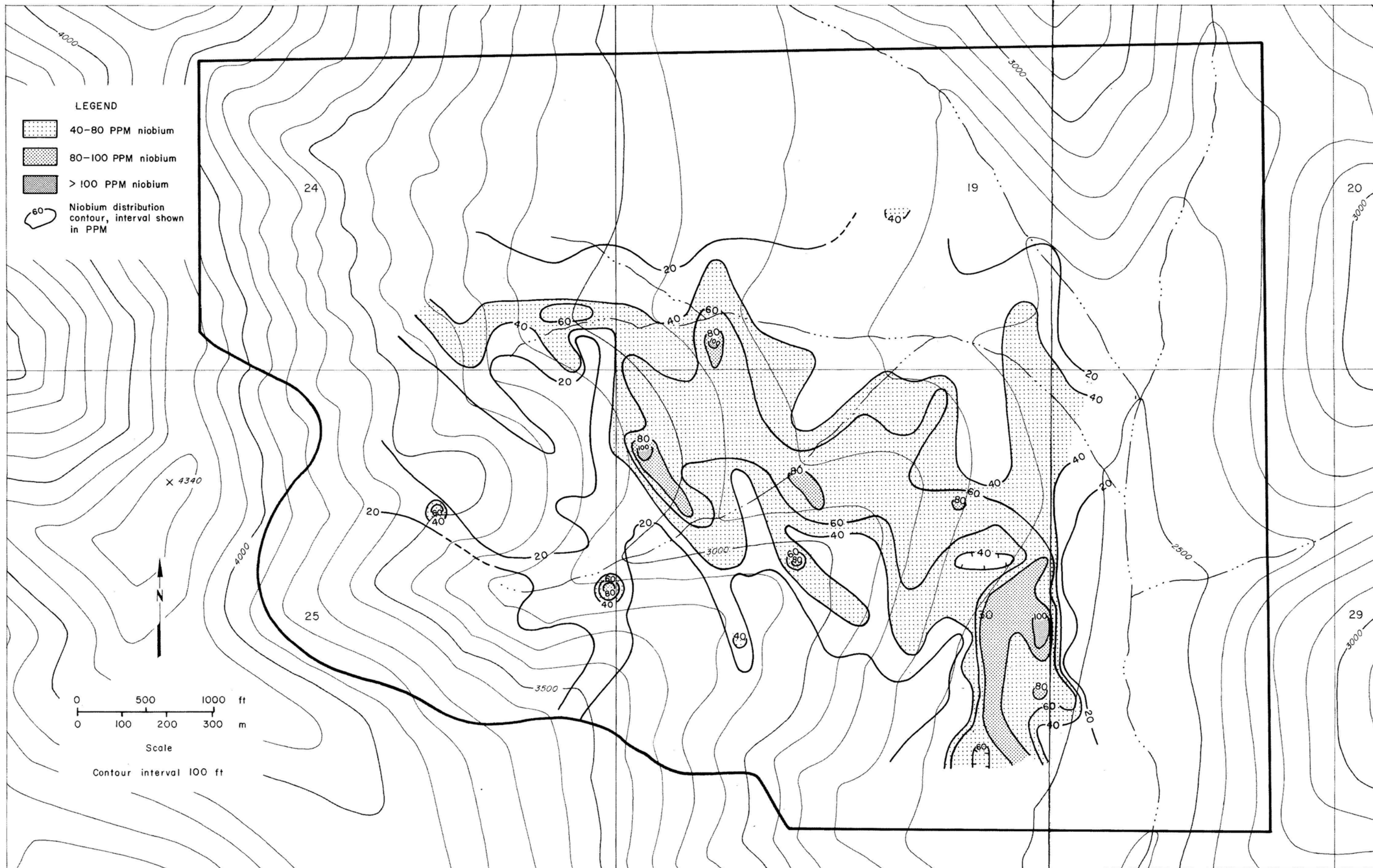


Figure 14. Distribution of niobium in soils.

comparison with molybdenum. Contour intervals for lead, molybdenum, and tungsten represent one-half and thereafter whole number multiples of these selected base levels. Niobium in soils was contoured at 60, 80, and 100 ppm. A niobium value of 60 ppm equals four times the average abundance given by Brooks (3).

The soil metal contents are zoned, with tungsten-rich soils partially coincident with higher elevations of the gossan zone and the topaz-bearing silicified Qp rocks, particularly in the vicinity of the base station knob. The tungsten-rich soils also correspond to the area where the VLF-EM survey shows the presence of conductive material. Higher molybdenum and to some extent niobium values are associated with the more intensely oxidized central portion of the gossan zone and the intrusive breccia. The combined area of anomalous tungsten and molybdenum soil values is enclosed by a zone of lead-rich soils that coincides with the peripheral metasedimentary rocks (Mcg and Pzp). This zonation is apparent by comparing figures 11 through 14, but it is shown more clearly by contouring the percent of soil molybdenum, lead, or tungsten where they are individually in excess of 50 pct of the combined total amount of these metals (fig. 15).

*** PLACER MINERALIZATION

Investigations by the authors in 1977 (1, 18) showed that the south-flowing drainage of the map area contained placer tungsten minerals. Heavy mineral concentrate (32.8 g) from a 2.5 ft³ bulk sample of alluvial gravel taken from the active stream bed approximately 2 miles downstream of the complex contained 3 pct W and 0.15 pct Nb.

Potential for placer tungsten was further confirmed by the presence of tungsten in heavy mineral concentrates collected during the present

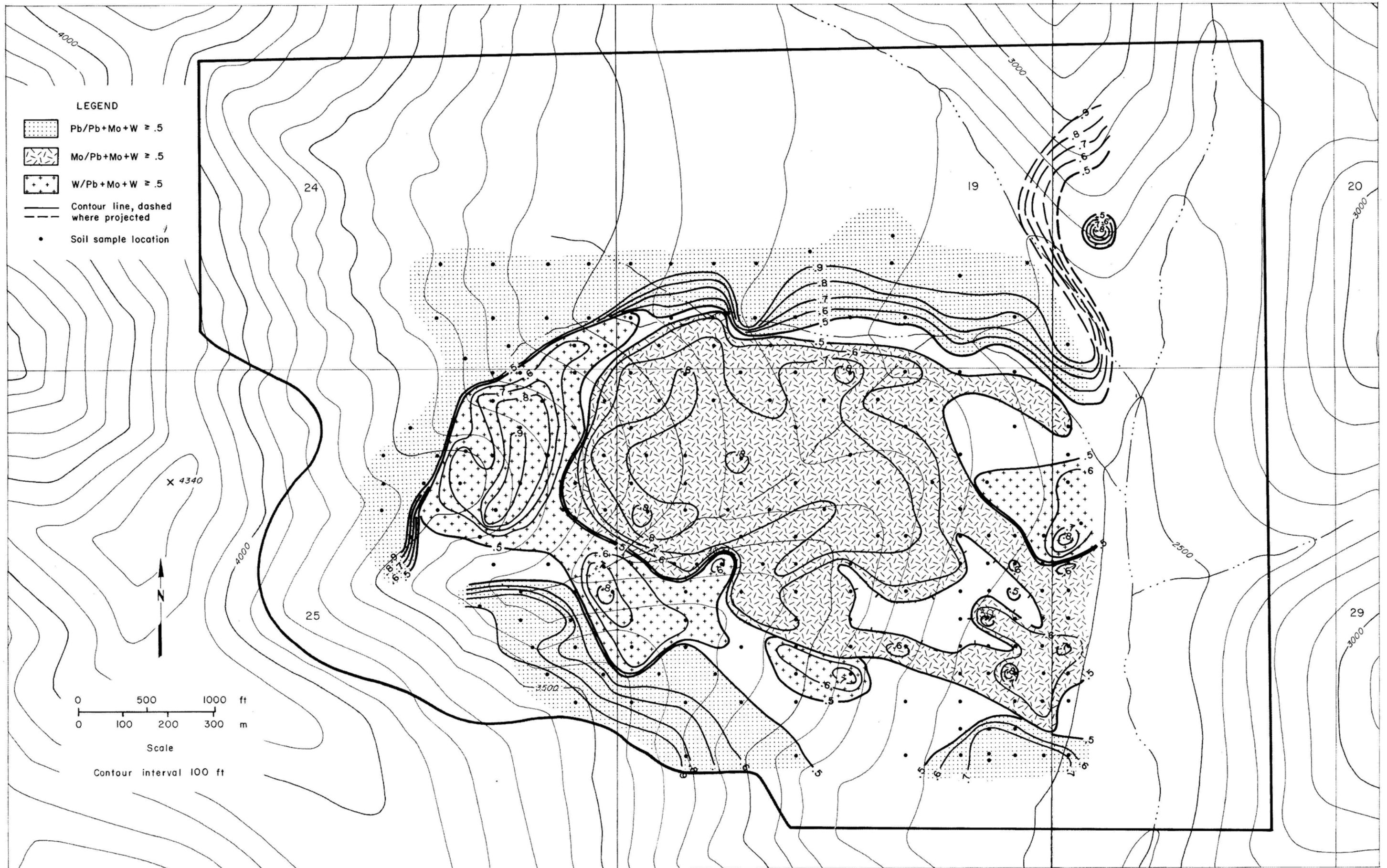


Figure 15. Zonation of lead, molybdenum, and tungsten expressed as a percentage of total metal content in soils.

study (fig. 3, and table 2). These concentrates were reduced from stream bed samples of surficial coarse gravel and clayey silt. Wolframite [(Fe, Mn) WO₄] was identified by microprobe analysis, and a zonal variation between the iron-rich end member ferberite and the manganese-rich end member huebnerite (samples 238P-240P) was apparent across individual grains. Many of the mineral grains were unaltered; however, others show partial alteration to iron oxide. Niobium was also detected (by microprobe analysis of sample 240P) in a pyrochlore-type mineral (NaCaNb₂O₆F) that occurred as inclusions in a titanium-rich host mineral. Samples 240P and 238P contained topaz and all of the samples contain minor amounts of pyrite, zircon, apatite, chlorite, monazite, and rutile. Pyrite was noted in sample 237P. No tin-bearing minerals were found.

TABLE 2. - Alluvial heavy mineral concentrates¹

Sample	Sample volume, ² ft ³	Weight of concentrate, g	Nb ₂ O ₅ , pct	Sn, pct	Ta ₂ O ₅ , pct	WO ₃ , pct	Estimated lb WO ₃ /yd ³
237P..	1.4	43.6	ND	ND	ND	ND	ND
238P..	1.8	110.8	0.035	ND	ND	10.3	0.50
239P..	1.4	376.4	ND	ND	ND	8.8	.38
240P..	2.3	119	ND	ND	ND	12.7	.521

ND Not detected.

¹Analyses by X-ray fluorescence, Bureau of Mines Reno (NV) Research Center.

²Volume includes a 25-pct swell factor deduction applied to the measured loose volume.

³Coarse wolframite occurs in sample 239P; some may have been lost during 0.25-in field screening.

The lighter minerals differ in the four concentrate samples. Sample 240P contains more quartz and iron oxides than the other three. An unidentified mineral phase containing aluminum, silicon, potassium, and varying amounts of iron is commonly present in all the samples but is more abundant in samples 240P and 238P. Also present in samples 238P and 240P is a phase containing sulfur, potassium, and iron, tentatively

identified as jarosite $[KFe_3(SO_4)_2(OH)_6]$. In samples 237P and 239P the principal light minerals appear to be epidote and various iron oxides. Clay was more abundant in the gravels in the two streams draining the intrusive center (samples 238P and 240P).

Outwash deposits containing quantities of wolframite and possible minor concentrations of niobium minerals have accumulated within the topographic bowl above the 2,500-ft elevation. Erosion of the bowl has resulted in transport of alluvium along the valley to the south (fig. 4) where tungsten was found in 1977. It would be expected therefore that unknown quantities of wolframite are contained within the alluvial gravels for at least several miles downstream. Estimates of grade and yardage are, however, not possible with only these few samples.

*** LODE MINERALIZATION

Molybdenum and tungsten occurrences are associated with the topaz-bearing, Qp and the northwest-trending gossan zone (fig. 7). Molybdenite has been identified at only one location, although some oxidized samples from the gossan zone contain as much as 0.8 pct Mo. Wolframite, however, was identified at several locations. Topaz and minor galena occurrences were found. Appendix B lists analytical results and descriptions of rocks analyzed from the grid area. Due to the total lack of unweathered bedrock exposures the extent and type of mineralization is inferred in part on the basis of rubble and on soil geochemistry.

Lead

Small amounts of galena are present in bleached, propylitically-altered metasedimentary rocks and gossan near sample location 1d in the extreme northwestern part of the map area (figs. 3 and 7). The galena occurs with clay as occasional crystals in quartz veinlets and in clay-filled

vugs.

Molybdenum

Molybdenite was observed as small flakes in Rp near sample location 202R (fig. 3) but was not observed elsewhere. Chips of unweathered porphyry containing minute metallic grains were separated after crushing of geochemical samples, and found to contain up to 8,700 ppm Mo. Mineral identity is unknown, however. Soil samples with molybdenum values in excess of 600 ppm (0.1 pct MoS₂ equivalent) occupy a 100 acre area and characterize most of the 1-mile long, northwest-trending gossan zone (figs. 5 and 11). Individual soil samples contain as much as 4,700 ppm Mo. Samples of leached porphyritic rocks with gossan contain up to 8,000 ppm Mo.

Within the gossan zone, the original sulfide minerals have been oxidized. Limonite, goethite, and hematite are the main iron-bearing oxides although in places, the sulfate jarosite is abundant. Locally the gossan is massive, and some is slaggy and silicified, indicating a period of oxidation prior to a later introduction of silica. More commonly, however, the oxide minerals occurs as fracture-fillings, in vugs and larger pockets, and form coarse boxwork structures in iron-stained and silicified porphyritic rocks. More massive gossan tends to occur in the axial portion of the zone and is generally more common in the eastern and western segments. By comparison, the central segment of the zone where it crosses the ridge line and then to the east is narrower and the amount of gossan is considerably less (fig. 5).

Tungsten

Euhedral crystals of wolframite up to 0.25 in long occur on drusy quartz that partially fills fractures in specimens of the silicified

bedrock near sample location 215R and at grid station 1000E-1000N. Wolframite also occurs as discrete zoned crystals within siliceous jarosite in fracture-fillings near sample location 215R (fig. 3). More commonly, finely disseminated wolframite (identified by XRD analyses) occurs in some of the porphyritic rocks (see samples 212R, 215R, 217R on fig. 3). It was observed principally in the west central area of the gossan zone and is commonly associated with topaz, rutile, and unidentified metallic minerals. These tungsten-bearing rocks occur within an area of about 60 acres where soils contain in excess of 500 ppm tungsten. Up to 5,000 ppm W was detected in individual soil samples. The area is located on the northern edge of the gossan zone and are more particularly associated with the Qp rocks peripheral to the gossan zone. This area is generally coincident with the conductive zone identified by the VLF-EM survey.

Sample 208R located near the northern edge of the complex and beyond the mapped gossan zone, was taken from one of the few sites where bedrock is exposed. A sample of rhyolite porphyry (208R), with a purple phyllosilicate (muscovite) groundmass and very finely disseminated opaque minerals contained 1,000 ppm W and 7,900 ppm Mo.

Niobium

The geologic association of niobium in soils to bedrock sources is uncertain when comparing figure 5 (local geology) to figure 14 (distribution of niobium in soils). A few grains of an unidentified niobium mineral were detected by microprobe examination of a sericite-quartz rock in sample location 208R and by X-ray diffraction analysis of 217R. Sample 208R also contained traces of barite, monazite, zircon, and rutile. There is a correlation of the higher niobium soil values (fig.

14) with the higher radiometric readings (fig. 8).

*** DISCUSSION

The Bear Mountain porphyry occurrence is within a high level, multi-phased intrusive complex that contains many features commonly associated with porphyry molybdenum deposits (16, 20, 23). Such deposits contrast with the copper-molybdenum porphyry, which are typically associated with granodiorite to quartz monzonite bodies. Various investigators have applied the term "Climax-type" in specific reference to the copper-deficient molybdenum deposits near Climax, CO (20-21, 23). Criteria of these deposits have been characterized as a deposit model. Similarities to Bear Mountain, while tentative at this stage, include geologic setting, alteration, trace element and mineralogic associations, mineral zonation, and age (age similarity may be merely coincidence rather than a geologic correlation).

Like Climax-type porphyry molybdenum deposits, the molybdenum-tungsten occurrence at Bear Mountain is associated with a siliceous, multi-phase complex of porphyritic igneous rocks, generally consisting of rhyolite and quartz porphyries that have intruded the intersection of two regional topographic linears. Bipyramidal quartz, a common feature of molybdenum deposits, is a constituent of the porphyritic rocks at Bear Mountain. Climax-type porphyry molybdenum deposits measure up to a square kilometer (250 acres) or less in size. The Bear Mountain complex is exposed over an area of approximately 275 acres; however, it is likely that the intrusive rocks are continuous below surficial cover with porphyry exposures 1,500 ft to the northeast. The complex may also extend under altered metasedimentary rocks for 2,000 ft to the northwest. Within this area soil geochemistry indicates anomalous molybdenum over 100 acres, with an

additional partially overlapping 60 acres of anomalous tungsten.

Like Climax-type porphyry molybdenum deposits, the Bear Mountain occurrence also contains evidence of zoned hydrothermal alteration. The Bear Mountain occurrence has an area of sericitic and argillic alteration that is overlain by a zone of silicification and topaz. Feldspar-destructive alteration lies outboard of this to the south. A halo of pyrite and propylitic alterations is also present along the margins of the stock, but because of lack of outcrop and leaching, the extent is unknown. The VLF-EM data suggest a conductive zone, possibly due to pyrite, is associated with or adjacent to the topaz-quartz porphyry zone along the western perimeter of the complex. The apparent lack of a potassic alteration zone may be explained by subsequent silicification, similar to that described by Wallace and others (22) in the high-silica rock underlying the upper ore body at Climax.

Common mineralogical and geochemical characteristics of the Climax-type molybdenum deposits include an association with tungsten as wolframite (usually huebnerite); fluorine-rich minerals such as mica, garnet, and most commonly fluorite; traces of tin as cassiterite; and trace amounts of niobium, tantalum, and uranium. The Bear Mountain occurrence was found to be particularly enriched in tungsten as wolframite. The data presently available indicates tungsten is nearly as abundant as molybdenum. Niobium is also present in minor amounts and tin was detected in some samples. Uranium was not evaluated. No fluorite was identified; however, fluorine is present in topaz.

Zinc and lead values typically form a halo around Climax-type deposits. Lead values occur in peripheral metasedimentary rocks at Bear Mountain.

No significant zinc enrichment was detected and copper is absent, if not depleted. At Climax, the molybdenum ore body is capped by a tungsten-pyrite zone which appears remarkably similar to the limonitic topaz-wolframite-bearing quartz porphyry phase at Bear Mountain. The molybdenum zone of 600 ppm Mo or greater in soils and rocks is associated with a gossan which lies below the quartz porphyry.

All of the Climax-type molybdenum deposits of the western United States cordillera are mid-Tertiary in age and younger than 50 m.y. Ludington (16), however, noted that ages were older to the north. A great distance intervenes between Bear Mountain and the Climax deposits and the correspondence in age of porphyry rocks at Bear Mountain is possibly fortuitous. However, location of Bear Mountain is similarly situated in the Alaska counterpart of the Colorado Front Ranges.

In an oxidizing environment chemical transport can be important for some metals including molybdenum, and the possibility of 'scavaging' of molybdenum by hydrous iron oxides may lead to false anomalies. However, Wallace (22), in discussion of molybdenum gossans in the Climax area of Colorado, concludes that oxidation of molybdenum results in neither significant enrichment, nor loss, of molybdenum. The recent periglacial history of the Climax area appears to be similar to the Bear Mountain area. While the presence of molybdenum at the Bear Mountain occurrence can only be inferred, if, as at Climax, there is no oxidation enrichment, then approximately 100 acres contain in excess of 600 ppm molybdenum, equivalent to approximately 0.1 % MoS_2 , and the economic cut-off grade is 0.20 %. Additionally, the upper ore body tungsten zone at Climax, Colorado, contains about 0.06 % WO_3 (500 ppm tungsten equivalent) in the richer parts.

The comparisons made above are preliminary. The similarities, however, indicate that the mineralization at Bear Mountain can be classified as a tungsten-rich, Climax-type, porphyry molybdenum occurrence. Most deposits of this type contain between 100 and 500 million tons of molybdenum ore and have a minimum cutoff grade of ± 0.1 pct MoS_2 where surface mining can be employed (16). Although it was not possible to systematically sample bedrock, soils containing the equivalent of 0.1 pct MoS_2 or greater extend over an area of 100 acres at Bear Mountain. Samples of gossaniferous rubble contained a similar level of molybdenum. Bear Mountain also contains substantial tungsten (greater than 0.06 pct WO_3 over 60 acres) and recovery of some byproduct niobium and locally tin may be possible.

*** CONCLUSION

Near Bear Mountain in Alaska, a multi-phased complex comprising rhyolite porphyry, quartz porphyry, and intrusive breccia contains molybdenum, tungsten, and associated mineralization. Within the exposed area of the complex (approximately 275 acres), soil geochemical results indicate that an area of approximately 100 acres contains values equal to or exceeding 600 ppm Mo. This area partially coincides with an area of 60 acres that contains soil values of at least 500 ppm W. These threshold values were arbitrarily selected because they are equivalent to 0.1 MoS_2 and 0.06 WO_3 . A grade of 0.1 MoS_2 is a commonly accepted lower limit in economic porphyry molybdenum deposits; 0.06 WO_3 represents the average grade of the tungsten zone at Climax, CO. Anomalous niobium values of 60 to 120 ppm are also present. The area of anomalous molybdenum soil values is approximately coincident with a zone of gossan. Argillic and sericitic alteration are pervasive throughout but especially so near the

mineralized area; silicification and topaz are common near the upper level of the complex. The surrounding metasedimentary rocks are propylitically altered, bleached, and silicified. A prominent zone of hematite staining occurs along the contact zone where exposed on the western margin. Comparison with Climax-type molybdenum deposits indicates numerous similarities to the occurrence at Bear Mountain. The Bear Mountain complex can be inferred to be a tungsten-rich, Climax-type porphyry molybdenum occurrence.

Surface sulfide minerals have been largely oxidized. Only one specimen contained visible molybdenite. Wolframite, however, including both the ferberite and huebnerite end members, occurs as disseminated grains in samples of porphyritic rock, in quartz veins, and in silicified gossan and indicates at least three modes of tungsten mineralization. Rock samples collected for analyses contained up to 0.8 pct Mo and 0.6 pct W. Some zonation is apparent between tungsten- and molybdenum-rich parts of the complex. Wolframite occurs as finely disseminated grains in topaz-bearing quartz porphyry in the western higher elevations of the complex where soil samples indicate low or nil molybdenum values. The underlying gossan zone in rhyolite porphyry and breccia also contains coarser-grained wolframite crystals; however, molybdenum soil values over the gossan are generally equal to or higher than the tungsten values. Lead values in the soil samples occur within metasedimentary rocks around the perimeter of the complex.

Placer samples containing approximately 0.5 lb of WO_3/yd^3 in surface gravels indicate placer tungsten deposits may occur in a large topographic depression into which the complex has been eroding. Analysis of a placer sample 2 miles downstream also indicated the presence of tungsten.

The Bear Mountain occurrence lies along an east-trending regional zone of anticlines and domes that extends about 50 miles to the west toward Table Mountain and into Canada to the east. Felsic igneous and basement metasedimentary rocks occur elsewhere along this zone which may be favorable for additional deposits; however, no known mineral exploration has been attempted. The area of Galena Creek which lies along this trend contains steeply dipping base metal veins and is especially recommended for further evaluation in light of the lead enrichment peripheral to the Bear Mountain porphyry occurrence.

*** REFERENCES

1. Barker, J. C. Mineral Investigations of Certain Lands in the Eastern Brooks Range: A Summary Report. BuMines OFR 63-78, 1978, 25 pp.
2. Barker, J. C. Mineral Investigations of Certain Lands in the Eastern Brooks Range, 1978. BuMines OFR 37-81, 1981, 288 pp.
3. Brooks, R. R. Geobotany and Biogeochemistry in Mineral Exploration. Harper & Row, 1972, 290 pp.
4. Brosge', W. P., U.S. Geol. Surv. Written communication, 1977, 1980, 1983, 1984; available upon request from J. C. Barker, BuMines, Fairbanks, AK.
5. Brosge', W. P., E. E. Brabb, and E. R. King. Geologic Interpretation of Reconnaissance Aeromagnetic Survey of Northeastern Alaska. U.S. Geol. Surv. Bull. 1271-F, 1970, pp. F1-F14.
6. Brosge', W. P., J. T. Dutro, Jr., M. D. Mangus, and H. N. Reiser. Paleozoic Sequence in the Eastern Brooks Range, Alaska. Am. Assoc. Petroleum Geol. Bull., v. 46, no. 12, 1962, pp. 2174-2198.
7. Brosge', W. P., and H. N. Reiser. Geochemical Reconnaissance Maps of Granitic Rocks, Coleen and Table Mountain Quadrangles, Alaska. U.S. Geol. Surv. OFR 323, 1968, 4 sheets.
8. Brosge', W. P., and H. N. Reiser. Geological Survey Research 1968. U.S. Geol. Surv. Prof. Paper 600-A, 1968, p. A41.
9. Brosge', W. P. and H. N. Reiser. Lead-Zinc Mineralization at Bear Mountain, Southeastern Brooks Range. In Accomplishments During 1976, (K. M. Blean, ed.). U.S. Geol. Surv. Circ. 751-B, 1977, pp. B8-B10.
10. Brosge', W. P., and H. N. Reiser. Preliminary Geologic and Mineral Resource Maps, Arctic National Wildlife Range, Alaska. U.S. Geol. Surv. Open File Map 76-539, 1976.

REFERENCES--Continued

11. Brosge', W. P., H. N. Reiser, J. T. Dutro, Jr., and R. L. Detterman. Reconnaissance Geologic Map of Table Mountain Quadrangle, Alaska. U.S. Geol. Surv. Open File Map 76-546, 1976.
12. Bryant, D. G. Intrusive Breccias Associated with Ore, Warren (Bisbee) Mining District, Arizona. Econ. Geol. and Bull. Soc. Econ. Geol., v. 63, 1968, pp. 1-12.
13. Dillon, John. Alaska Div. of Geol. and Geophysical Surveys. Written communication, February, 1984; available upon request from J. C. Barker, BuMines, Fairbanks, AK.
14. Dutro, J. T., Jr., W. P. Brosge', and H. N. Reiser. Significance of Recently Discovered Cambrian Fossils and Reinterpretation of the Neruokpuk Formation, Northeastern Alaska. Amer. Assoc. Petroleum Geol. Bull., v. 56, no. 4, 1972, pp. 808-815.
15. Fraser, D. C. Contouring of VLF-EM data. Geophysics, v. 34, no. 6, 1969, pp. 958-967.
16. Ludington, S. Granite Molybdenite Systems. Ch. in Characteristics of Mineral Deposit Occurrences. U.S. Geol. Surv. OFR 82-795, 1982, pp. 43-46.
17. Reed, B. L. Geology of the Lake Peters Area, Northeastern Brooks Range, Alaska. U.S. Geol. Surv. Bull. 1236, 1968, 132 pp.
18. Resource Exploration Consultants, Inc. Geology, Geochemistry and Mineralization in the Bear Mountain Area, Eastern Brooks Range, Alaska. Appendix in BuMines OFR 37-81, 1981, pp. 106-137.
19. Sable, E. G. Geology of the Western Romanzof Mountains, Brooks Range, Northeastern Alaska. U.S. Geol. Surv. Prof. Paper 897, 1977, 81 pp.

REFERENCES--Continued

20. Theobald, P. K., Jr. Characteristics of the Colorado-Type (Climax Type) Molybdenum Deposits Readily Recognized at the Surface. Ch. in Characteristics of Mineral Deposit Occurrences. U.S. Geol. Surv. OFR 82-795, 1982, pp. 47-48.
21. Theodore, T. G. Preliminary Model Outline for Fluorine-Deficient Porphyry Molybdenum Deposits. Ch. in Characteristics of Mineral Deposit Occurrences. U.S. Geol. Surv. OFR 82-795, 1982, pp. 37-42.
22. Wallace, S. R., N. K. Muncaster, D. C. Jonson, W. B. MacKenzie, A. A. Bookstrom, and V. E. Surface. Multiple Intrusion and Mineralization at Climax, Colorado. Ch. in Ore Deposits of the United States, ed. by J. D. Ridge. AIME, v. 1, 1968, pp. 606-641.
23. White, W. H., A. A. Bookstrom, R. J. Kamilli, M. W. Ganster, R. P. Smith, D. E. Rarta, and R. C. Steininger. Character and Origin of Climax-Type Molybdenum Deposits. Econ. Geol. and Bull. Soc. Econ. Geol., 75th anniv. v., 1981, pp. 270-316.

*** APPENDIX A.--SOIL SAMPLES AND ANALYTICAL RESULTS

Sample	Ag, ppm	Au, ppm	Mo, ppm	Nb, ppm	Pb, ppm	Sn, ppm	W, ppm	Site description
1d..	NA	NA	ND	ND	1,680	55	60	Hematitic, clayey silt on scree slope.
2d..	NA	NA	ND	ND	120	70	16	Limonitic, clayey silt from a frost boil.
3d..	1.0	ND	4.8	16	1,600	7	ND	Limonitic soil from talus fan at base of gully.
4d..	ND	ND	6.7	60	320	ND	12	Red-brown, clayey silt and gravel from frost boil.
5d..	NA	NA	ND	ND	53	16	240	Limonitic, clayey silt from a frost boil.
6d..	2.0	ND	9.4	6.3	3,000	ND	ND	Red-brown, clayey silt at base of prominent outcrop in talus slope.
7d..	ND	ND	ND	30	360	ND	6	Brown, clayey silt from frost boil in solifluction area.
8d..	2.377	ND	24	36	2,200	ND	8	Dark brown, silty soil from talus slope.
9d..	1.0	ND	ND	19	1,100	5	ND	Brown, clayey silt from frost boil in tundra.
10d..	ND	ND	1.5	32	1,300	ND	6	Do.
11d..	1.0	ND	ND	21	1,400	ND	8	Do.
12d..	1.0	ND	ND	17	1,400	ND	6	Yellow-brown, clayey silt from frost boil in tundra.
13d..	0.96	ND	21	42	1,100	ND	6	Do.
14d..	.99	ND	4.1	25	1,200	ND	6	Silty sand and alluvial gravel overlain by tundra.
15d..	ND	ND	12	20	340	ND	16	Brown, clayey silt from frost boil in tundra.
16d..	.710	ND	13	39	630	ND	7	Do.
17d..	ND	ND	4.0	20	340	ND	16	Do.
18d..	ND	ND	2.5	22	370	ND	8	Do.
19d..	ND	ND	30	59	760	ND	24	Brown, clayey silt from frost boil.
20d..	ND	ND	10	46	240	ND	ND	Dark brown, silty soil from talus slope.
21d..	ND	ND	14	60	1,900	ND	ND	Brown, clayey silt from frost boil in tundra.
22d..	ND	ND	19	72	1,500	ND	ND	Gray-brown soil from frost boil.
23d..	ND	ND	140	40	350	ND	600	Brown, silty sand from frost boil in tundra.
24d..	ND	ND	340	29	490	ND	400	Red-brown, clayey silt from frost boil in tundra.
25d..	ND	ND	1,300	62	250	ND	320	Yellow-brown, clayey silt from frost boil in tundra.
26d..	ND	ND	15	22	740	ND	40	Do.
27d..	ND	ND	87	27	370	ND	160	Do.
28d..	ND	ND	280	35	360	ND	600	Sandy, alluvial gravel overlain by tundra.
29d..	ND	ND	200	34	370	ND	120	Do.
30d..	ND	ND	150	51	610	ND	60	Brown, sandy soil from frost boil in tundra.
31d..	ND	ND	ND	24	1,200	ND	6	Brown, clayey silt from frost boil.
32d..	ND	ND	30	10	290	16	600	Red clay from frost boil in solifluction area.

See explanatory notes at end of table.

Sample	Ag, ppm	Au, ppm	Mo, ppm	Nb, ppm	Pb, ppm	Sn, ppm	W, ppm	Site description
33d..	ND	ND	560	29	310	9	1,200	Red-brown, clayey silt from frost boil.
34d..	ND	ND	1,400	56	70	8	600	Red clay from frost boil in solifluction area.
35d..	ND	ND	1,600	110	310	ND	200	Brown, clayey silt from frost boil in solifluction area.
36d..	ND	ND	1,200	41	210	7	320	Do.
37d..	ND	ND	35	2.6	420	11	12	Gray-brown, clayey silt from frost boil in tundra.
38d..	ND	ND	12	59	930	ND	ND	Brown, clayey silt from frost boil.
39d..	ND	ND	ND	19	480	ND	28	Dark brown soil from frost boil.
40d..	ND	ND	350	19	370	7	800	Red-brown, clayey silt from frost boil.
41d..	ND	ND	690	17	57	6	1,000	Do.
42d..	ND	ND	1,000	78	35	5	320	Do.
43d..	ND	ND	640	51	57	ND	80	Sandy, clayey silt from frost boil.
44d..	ND	ND	420	66	120	ND	100	Red-brown, silty clay from frost boil in solifluction area.
45d..	ND	ND	460	46	86	6	60	Do.
46d..	ND	ND	1,900	28	170	12	120	Red-brown, silty clay and rounded alluvial gravel.
47d..	ND	ND	450	35	120	6	160	Red-brown, silty sand.
48d..	ND	ND	290	28	150	ND	160	Gray-brown, silty soil in frost boil.
49d..	ND	ND	350	41	170	6	160	Red-brown, clayey silt from frost boil in tundra.
50d..	ND	ND	3.0	21	150	12	600	Red-brown silt from frost boil.
51d..	ND	ND	470	ND	210	8	3,000	Red-brown, clayey silt from frost boil.
52d..	ND	ND	1,700	38	ND	6	800	Do.
53d..	ND	ND	2,200	77	46	ND	800	Red-brown clay from frost boil.
54d..	ND	ND	940	75	120	ND	160	Red-brown, sandy silt from frost boil.
55d..	ND	ND	640	51	78	ND	280	Red-brown, silty clay from frost boil in solifluction area.
56d..	ND	ND	610	29	160	8	100	Red-brown, silty clay from frost boil.
57d..	ND	ND	300	56	94	ND	120	Brown, clayey, silty sand from frost boil.
58d..	ND	ND	150	70	89	ND	60	Brown, silty sand in frost-fractured rubble.
59d..	ND	ND	8.0	10	300	ND	ND	Brown, clayey silt from frost boil.
60d..	ND	ND	120	36	87	17	3,000	Brown, sandy soil from scree slope.
61d..	ND	ND	1,400	ND	97	7	2,000	Red, sandy clay from frost boil.
62d..	ND	ND	2,900	57	78	8	600	Red, clayey silt from frost boil.
63d..	0.750	ND	980	36	270	ND	60	Red-brown soil from frost boil in solifluction area.
64d..	ND	ND	290	56	140	ND	40	Brown, silty sand from frost boil on scree slope.
65d..	ND	ND	170	55	80	ND	132	Brown, clayey silt from frost boil.
66d..	ND	ND	520	46	150	ND	200	Brown soil with alluvial gravel from frost boil.

See explanatory notes at end of table.

Sample	Ag, ppm	Au, ppm	Mo, ppm	Nb, ppm	Pb, ppm	Sn, ppm	W, ppm	Site description
67d..	ND	ND	3.1	35	150	ND	ND	Brown soil from tundra slope.
68d..	ND	ND	18	7.1	270	ND	60	Very hematitic, clayey silt from unvegetated saddle.
69d..	2.028	ND	4.5	ND	380	52	1,000	Yellow, clayey soil from steep scree slope.
70d..	2.172	ND	8.9	ND	260	45	600	Very hematitic, silty clay on sidehill.
71d..	ND	ND	290	21	69	12	2,000	Brown, sandy soil from scree slope.
72d..	ND	ND	2,700	36	49	ND	600	Brown, sandy silt from sidehill rubble.
73d..	ND	ND	3,400	120	180	ND	1,000	Red-brown, clayey silt from frost boil.
74d..	ND	ND	1,400	71	63	ND	320	Do.
75d..	ND	ND	2,600	61	160	ND	200	Red-brown, clayey silt from frost boil in solifluction area.
76d..	ND	ND	290	67	54	ND	40	Brown, silty sand from frost boil on scree slope.
77d..	ND	ND	ND	110	58	18	100	Sandy soil in solifluction lobe.
78d..	ND	ND	210	50	99	ND	160	Brown, clayey silt from frost boil in solifluction area.
79d..	ND	ND	5.5	6.7	430	ND	ND	Brown, clayey silt from frost boil in tundra area.
80d..	ND	ND	ND	ND	210	10	100	Yellow, clayey silt in unvegetated saddle.
81d..	0.950	ND	1.7	ND	320	54	800	Yellow-red, clayey silt in un-vegetated saddle.
82d..	ND	ND	120	15	86	21	2,000	Brown, clayey silt from talus slope.
83d..	ND	ND	3,100	ND	110	20	2,000	Red-brown, clayey silt from talus slope.
84d..	ND	ND	2,700	33	65	15	500	Red-brown, clayey silt from frost boil.
85d..	ND	ND	2,600	50	76	10	600	Red-brown, clayey silt from frost boil in solifluction area.
86d..	ND	ND	440	24	85	ND	60	Brown soil with rounded alluvial gravel.
87d..	ND	ND	870	81	170	ND	100	Brown, clayey silt from frost boil.
88d..	ND	ND	300	63	43	ND	60	Tan, clayey silt from frost boil in rubble area.
89d..	ND	ND	240	42	32	ND	60	Clayey, brown soil from frost boil.
90d..	ND	ND	220	36	ND	ND	320	Do.
91d..	ND	ND	280	23	ND	ND	600	Brown, clayey silt from frost boil in tundra.
92d..	ND	ND	ND	23	92	ND	5	Brown silt from frost boil.
93d..	ND	ND	24	7.9	160	10	240	Deep red, clayey silt from un-vegetated saddle.
94d..	ND	ND	80	ND	92	14	5,000	Brown, sandy soil from scree slope.
95d..	ND	ND	650	26	160	18	1,000	Brown, sandy silt from sidehill rubble.
96d..	ND	ND	3,200	34	270	13	800	Red-brown, clayey silt from un-vegetated solifluction area.
97d..	ND	ND	4,700	22	130	ND	320	Do.
98d..	ND	ND	3,400	93	200	5	360	Do.
99d..	ND	ND	2,000	55	190	ND	400	Brown, clayey silt underlying rubble slope.

See explanatory notes at end of table.

Sample	Ag, ppm	Au, ppm	Mo, ppm	Nb, ppm	Pb, ppm	Sn, ppm	W, ppm	Site description
100d..	ND	ND	930	57	180	ND	160	Brown, silty sand underlying rubble slope.
101d..	ND	ND	380	89	85	ND	160	Brown clayey silt from frost boil on scree slope.
102d..	ND	ND	580	82	80	5	400	Light brown, sandy soil from frost boil.
103d..	SL	SL	SL	SL	SL	SL	SL	Brown, clayey silt from frost boil in tundra.
104d..	ND	ND	ND	18	78	ND	6	Brown, clayey silt from frost boil.
105d..	2.032	ND	160	ND	220	18	1,000	Red, silty clay in talus.
106d..	NA	NA	1,250	180	69	14	700	Red-brown soil from frost boil.
107d..	ND	ND	490	34	52	ND	200	Brown, silty soil from frost boil.
108d..	ND	ND	510	47	ND	ND	180	Do.
109d..	ND	ND	680	76	87	ND	200	Red-brown, sandy soil from solifluction lobe.
110d..	ND	ND	320	65	58	ND	280	Brown, sandy soil from frost boil on solifluction lobe.
111d..	ND	ND	510	57	69	ND	400	Clayey, brown soil from frost boil.
112d..	ND	ND	530	72	130	ND	240	Brown silt from frost boil.
113d..	ND	ND	170	58	150	8	400	Red-brown, loose silt from frost fractured rubble.
114d..	ND	ND	150	30	ND	19	1,000	Clayey, light brown soil from frost boil in tundra.
115d..	0.96	ND	1,100	21	320	15	320	Hematitic soil from frost boil.
116d..	1.00	ND	1,700	36	520	10	1,200	Red-brown, sandy soil from solifluction lobe.
117d..	ND	ND	290	25	370	15	1,760	Red-brown, sandy soil from frost boil.
118d..	ND	ND	500	10	66	16	1,000	Brown, silty sand underlying gossan rubble.
119d..	ND	ND	410	7.6	260	17	600	Do.
120d..	ND	ND	610	18	65	ND	280	Do.
121d..	ND	ND	550	42	44	8	1,000	Do.
122d..	ND	ND	1,300	35	59	ND	600	Red-brown, silty sand from frost boil on rubble slope.
123d..	ND	ND	1,200	45	95	ND	320	Red, sandy soil from frost boil in tundra area.
124d..	ND	ND	260	27	ND	ND	160	Red-brown, clayey silt from frost boil.
125d..	ND	0.017	290	45	ND	ND	140	Soil from frost boil in frost-fractured rubble field.
126d..	ND	ND	230	40	51	ND	200	Loose, tan-colored soil from scree slope.
127d..	NA	NA	330	38	94	ND	100	Brown silt from frost boil.
128d..	ND	ND	310	90	230	6	200	Red-brown, clayey silt from frost boil in tundra area.
129d..	ND	0.017	230	ND	ND	ND	70	Red-brown frozen soil from bog area.
130d..	ND	ND	2.3	ND	120	ND	8	Yellow-stained, clayey silt from frost boil on scree slope.
131d..	ND	ND	6.5	17	110	ND	18	Brown-yellow, clayey silt from frost boil at base of steep slope.
132d..	ND	ND	17	25	82	ND	60	Brown soil from frost boil.
133d..	ND	ND	180	8.8	30	16	1,200	Brown, silty sand underlying gossan rubble.

See explanatory notes at end of table.

Sample	Ag, ppm	Au, ppm	Mo, ppm	Nb, ppm	Pb, ppm	Sn, ppm	W, ppm	Site description
134d..	ND	ND	210	6.7	36	ND	280	Brown soil from frost boil in rubble slope.
135d..	ND	ND	540	4.3	73	ND	200	Hematitic, clayey silt.
136d..	0.89	ND	250	16	32	ND	200	Brown-red, clayey silt from frost boil.
137d..	ND	ND	360	28	ND	ND	280	Red-brown, sandy silt from frost boil.
138d..	ND	ND	570	60	65	8	400	Yellow-brown, sandy soil from small frost boils on rubble slope.
139d..	ND	0.016	340	51	170	6	320	Red-brown sandy soil from frost boil on solifluction lobe.
140d..	ND	ND	410	44	88	8	320	Brown soil from frost boil in solifluction area.
141d..	ND	ND	420	82	110	5	600	Brown silt from frost boil.
142d..	ND	ND	250	62	110	ND	100	Brown, clayey silt from frost boil.
143d..	NA	NA	99	ND	ND	6	40	Organic-rich frozen silty sand.
144d..	ND	ND	10	28	130	ND	7	Brown, sandy silt underlying scree slope.
145d..	NA	NA	2	ND	50	8	ND	Yellow-brown, clayey silt from mud flow on steep hillside.
146d..	ND	ND	11	10	85	16	240	Brown soil from frost boil in rubble slope.
147d..	ND	ND	91	19	73	ND	320	Do.
148d..	ND	ND	420	13	46	ND	200	Sandy silt from frost boil on scree slope.
149d..	ND	ND	410	54	85	ND	320	Brown, silty sand from solifluction lobe.
150d..	ND	ND	450	49	200	10	600	Sandy, hematitic soil from frost boil.
151d..	ND	ND	1,800	97	530	9	280	Red-brown, clayey silt from frost boil in solifluction area.
152d..	.69	ND	1,100	82	420	7	320	Red-brown, clayey silt from frost boil in tundra.
153d..	ND	ND	590	110	430	12	280	Do.
154d..	ND	ND	500	27	210	9	200	Do.
155d..	ND	ND	14	11	140	ND	12	Hematitic, clayey silt on steep hillside.
156d..	ND	ND	13	ND	65	8	24	Yellow, clayey silt from mud flow on steep hillside.
157d..	ND	ND	11	20	50	18	140	Red-brown, clayey silt from small frost boil in rubble slope.
158d..	ND	.014	6.0	16	46	5	36	Red-brown, sandy soil from frost boil.
159d..	ND	ND	43	40	72	12	100	Do.
160d..	ND	ND	34	3.4	ND	ND	110	Brown, clayey silt on scree slope.
161d..	ND	ND	580	31	70	9	360	Brown, silty sand from solifluction lobe.
162d..	ND	ND	480	44	34	ND	240	Red-brown soil from frost boil on terrace above the steep scree slope.
163d..	ND	ND	340	15	150	24	400	Sandy, hematitic soil from frost boil.
164d..	ND	ND	1,000	98	550	9	310	Red-brown, clayey silt from frost boil in solifluction area.
165d..	ND	ND	410	64	370	9	280	Red-brown, clayey silt from frost boil in tundra.
166d..	ND	ND	840	100	390	11	160	Do.

See explanatory notes at end of table.

Sample	Ag, ppm	Au, ppm	Mo, ppm	Nb, ppm	Pb, ppm	Sn, ppm	W, ppm	Site description
167d..	1.00	ND	1,300	34	270	6	200	Brown, frozen, sandy soil from bog area.
168d..	ND	0.026	3.9	17	210	ND	6	Soil from gully draining pyritic metasediments.
169d..	0.90	ND	14	22	93	ND	16	Red-brown, clayey silt from frost boil on ridge.
170d..	ND	ND	3.6	7.6	ND	ND	8	Sandy silt from scree slope.
171d..	ND	.019	12	8.6	47	5	28	Red-brown soil in talus.
172d..	ND	ND	44	ND	ND	10	100	Brown, clayey silt on scree slope.
173d..	.83	ND	140	12	51	8	600	Red-brown, silty sand on scree slope.
174d..	ND	ND	340	44	100	162	240	Sandy, red-brown silt from frost boil in tundra.
175d..	ND	ND	790	88	390	11	360	Red-brown clayey silt from frost boil in solifluction area.
176d..	ND	ND	2,300	67	400	9	160	Red-brown, clayey silt from frost boil in tundra.
177d..	ND	ND	740	75	290	11	200	Do.
178d..	ND	ND	820	13	360	11	200	Red-brown, clayey silt from frost boil.
179d..	ND	ND	1.2	34	130	ND	8	Soil from frost boil on ridge.
180d..	ND	ND	5.1	12	47	ND	6	Brown soil from frost boil.
181d..	ND	ND	4.8	11	ND	ND	8	Brown silt from scree slope.
182d..	ND	ND	15	11	40	ND	16	Brown soil from scree slope.
183d..	ND	ND	58	8.9	32	11	60	Red-brown soil from frost boil.
184d..	ND	ND	180	16	76	6	120	Red-brown, sandy soil from frost boil.
185d..	ND	ND	180	30	140	7	60	Dark brown, sandy silt from frost boil in tundra.
186d..	.76	ND	590	75	410	ND	120	Red-brown, clayey silt from frost boil in tundra.
187d..	.82	ND	1,000	81	420	18	120	Soil from frost boil.
188d..	ND	ND	370	67	280	ND	360	Brown, organic-rich, frozen, sandy soil.
189d..	ND	ND	130	27	130	ND	40	Red-brown, sandy silt from frost boil on solifluction lobe.
190d..	.74	ND	130	85	750	ND	60	Brown, clayey silt from frost boil.
191d..	ND	ND	140	70	480	7	60	Brown frozen silty sand from bog area.
192d..	ND	ND	1.9	13	100	ND	ND	Brown silt from scree slope.
193d..	ND	ND	27	12	67	ND	32	Dry, silty sand on scree slope.
194d..	ND	ND	160	25	170	8	160	Light brown, limonitic soil from frost boil on solifluction lobe.
195d..	.77	ND	120	17	400	ND	110	Do.
196d..	1.0	ND	280	76	830	10	60	Red-brown, clayey silt from frost boil in solifluction area.
197d..	ND	ND	120	15	46	ND	80	Red-brown soil from frost boil in solifluction area.
198d..	2.0	ND	280	93	840	7	60	Red-brown, clayey silt from frost boil in solifluction area.
199d..	1.00	ND	120	38	480	7	60	Brown, organic-rich, frozen sandy soil.
200d..	1.00	ND	110	28	520	9	40	Do.

NA Not analyzed.
ND Not detected.
SL Sample lost in lab.

NOTE.--See figure 3 for sample location.

*** APPENDIX B.--ROCK SAMPLE DESCRIPTIONS AND ANALYTICAL RESULTS

Sample	Ag, ppm	Au, ppm	Cu, ppm	F, ppm	Mo, ppm	Sn, ppm	Ta, ppm	W, ppm	Zn, ppm	Description
201R..	ND	ND	ND	240	23	ND	ND	14	ND	Rhyolite porphyry with banded silica. Rock contains clear, doubly terminated quartz phenocryst, green and purple phyllosilicate as clots replacing K-feldspar, and argillic alteration. Plagioclase as a major mineral with minor muscovite and hematite(?). ¹
202R..	ND	ND	ND	530	140	ND	ND	14	ND	Silicified and argillically altered rhyolite porphyry with clots and streaks of purple phyllosilicate replacing K-feldspar phenocryst and groundmass. Quartz and muscovite are the major minerals with minor plagioclase and trace kaolinite. ¹
203R..	ND	ND	ND	1,000	60	19	ND	10	ND	Rhyolite porphyry with finely disseminated purple phyllosilicates. Rock is cut by quartz veinlets with black metallics.
204R..	ND	ND	ND	NA	270	ND	ND	160	ND	Rhyolite (?) porphyry with leached, limonitic quartz stockworks. Abundant quartz, muscovite, and minor hematite. ¹
205R..	ND	ND	ND	4,100	180	ND	ND	200	ND	Quartz porphyry with yellow oxide-coated vugs. Limonitic and leached quartz veinlets cut rock. Major quartz and muscovite and minor topaz. ¹
206R..	ND	ND	ND	NA	NA	NA	ND	NA	ND	Pyritic siltstone.
207R..	ND	ND	ND	800	52	ND	ND	20	ND	Rhyolite porphyry with some clay alteration and magnetite crystals. Potassic feldspar phenocrysts are little altered; considerable muscovite in groundmass with minor kaolinite. ¹
208R..	0.67	ND	110	NA	7,900	11	ND	1,000	ND	Rhyolite porphyry with argillic alteration of the groundmass and streaks of green and purple phyllosilicate, sometimes bordering goethite and limonitic fractures. Minor topaz and muscovite. ¹ Microprobe examination detected traces of an unidentified niobium mineral plus barite, monazite, zircon, and rutile.
209R..	ND	ND	ND	NA	170	12	ND	280	ND	Rhyolite porphyry with slight argillic alteration and unidentified black metallics in clay vugs. Major minerals are quartz and muscovite, with minor K-feldspar and traces of kaolinite. ¹

See explanatory notes at end of table.

Sample	Ag, ppm	Au, ppm	Cu, ppm	F, ppm	Mo, ppm	Sn, ppm	Ta, ppm	W, ppm	Zn, ppm	Description
210R..	ND	ND	ND	NA	NA	NA	ND	70	ND	Silicified and brecciated meta-siltstone with disseminated black metallica.
211R..	ND	ND	ND	NA	220	NA	ND	600	ND	Limonite-goethite gossan and rhyolite porphyry breccia fragments.
212R..	ND	ND	ND	22,000	640	6	ND	360	ND	Quartz porphyry with argillic alteration, leached fractures and vugs, and minor boxwork. Some cavities coated with jarosite. Abundant quartz, topaz, and minor jarosite, wolframite, and muscovite. ¹
213R..	ND	ND	ND	NA	1,220	ND	ND	2,000	ND	Goethite-limonite gossan in relic rhyolite porphyry.
214R..	ND	ND	ND	NA	240	ND	ND	400	ND	Quartz porphyry with sericitic and argillic alteration, boxwork vugs, yellow oxide (jarosite?) coatings, and minute black metallic grains. Major quartz and topaz with traces of muscovite. ¹
215R..	7.08	ND	ND	NA	1,900	NA	ND	6,000	ND	Limonite-goethite gossan, rhyolite porphyry breccia fragments, and jarosite coatings and clots. Abundant quartz and jarosite with minor wolframite and feldspar. ¹
216R..	ND	ND	ND	840	120	6	ND	12	ND	Quartz porphyry with manganese oxide coatings. Major quartz and muscovite with minor K-feldspar, and traces of kaolinite. ¹
217R..	ND	ND	ND	NA	6,700	28	ND	3,000	ND	Goethite-limonite gossan with silicic skeletal structures. Minor rutile, topaz, and hematite. ¹ Finely disseminated wolframite tentatively identified.
218R..	ND	ND	70	NA	5,000	NA	66	1,000	ND	Rhyolite porphyry with limonite-stained fracture leaching, and boxwork cavities.
219R..	ND	ND	ND	NA	6,700	6	ND	600	ND	Goethite gossan; minor rutile and topaz. ¹
220R..	ND	ND	ND	NA	1,600	NA	ND	400	ND	Slaggy limonite-goethite gossan with jarosite (?) coatings and clots.
221R..	ND	ND	ND	NA	5,300	NA	ND	320	ND	Limonite-goethite gossan.
222R..	.37	ND	100	NA	7,000	12	ND	800	ND	Massive limonite-goethite gossan with relic rhyolite porphyry breccia fragments.
223R..	ND	ND	ND	NA	8,000	NA	ND	240	ND	Gossaniferous porphyry.

See explanatory notes at end of table.

Sample	Ag, ppm	Au, ppm	Cu, ppm	F, ppm	Mo, ppm	Sn, ppm	Ta, ppm	W, ppm	Zn, ppm	Description
224R..	ND	ND	ND	NA	1,800	NA	ND	ND	ND	Argillic altered rhyolite porphyry with limonite staining and intermittent boxwork cavities. Minor muscovite and feldspar. ¹
225R..	ND	ND	ND	200	210	NA	ND	400	ND	Relatively unaltered rhyolite porphyry with faint purple phyllosilicate in the groundmass. Limonite coatings on a few open fractures.
226R..	ND	ND	ND	NA	NA	NA	ND	NA	ND	Vuggy, sheared, fine-grained quartzite to metasiltstone with garnet, epidote, and trace sericitic and argillic alteration. Rock is cut by thin stringers of aplitic quartz porphyry containing an unidentified cryptocrystalline translucent orange-yellow mineral.
227R..	ND	ND	67	NA	4,300	9	ND	600	ND	Intrusive breccia with rounded to angular fragments of rhyolite, rhyolite porphyry, and metasedimentary rock. Goethite-limonite fracture fillings. Some kaolinite and black quartz in some clasts. ¹
228R..	NA	NA	ND	NA	NA	11	ND	NA	ND	Goethite-limonite gossan with relic quartz phenocrysts.
229R..	ND	ND	ND	NA	820	NA	ND	1,000	ND	Rhyolite porphyry with argillic alteration and discontinuous quartz veinlets up to 0.25 in thick. Major minerals are quartz and muscovite with minor topaz, and trace K-feldspar and kaolinite. ¹
230R..	NA	NA	ND	NA	2	9	ND	3	ND	Argillically altered rhyolite porphyry with trace muscovite and pyrite. Quartz phenocrysts embayed by groundmass.
231R..	ND	ND	ND	NA	2,800	NA	ND	320	ND	Limonite-goethite gossan and boxwork; minor feldspar, hematite, and garnet. ¹
232R..	ND	ND	ND	1,500	ND	NA	ND	ND	ND	Argillically altered rhyolite porphyry with red and yellow oxide coatings. Rock has a scoriaceous texture due to weathering and removal of feldspar phenocrysts and possibly pyrite. Quartz and muscovite with traces of potassic feldspar. ¹

See explanatory notes at end of table.

Sample	Ag, ppm	Au, ppm	Cu, ppm	F, ppm	Mo, ppm	Sn, ppm	Ta, ppm	W, ppm	Zn, ppm	Description
233R..	NA	NA	ND	NA	4	16	ND	3	ND	Argillically altered rhyolite porphyry with doubly terminated quartz phenocrysts, clay and muscovite after feldspar, and trace pyrite. Yellow oxide coatings. Trace plagioclase as phenocrysts.
234R..	ND	ND	ND	NA	ND	ND	ND	60	ND	Quartz porphyry with few relic feldspar phenocryst altered to clay and muscovite. Quartz phenocrysts are rounded. Open-space cavities with yellow oxide. Rock occurs in narrow zones cutting metasiltstone.
235R..	ND	ND	ND	NA	140	6	ND	140	ND	Limonite-goethite gossan with limonite-filled boxwork and relic siliceous structure. Gossan zone is 2 to 10 ft wide and hosted by rhyolite porphyry.
236R..	ND	ND	ND	NA	NA	NA	ND	NA	ND	Rhyolite porphyry with sericitic alteration of potassic feldspar ground-mass. Quartz phenocrysts are bi-pyramidal. Major minerals are quartz and muscovite. ¹

NA Not analyzed.

ND Not detected.

¹Identified by XRD. X-ray diffraction analyses by W. Barry, analyst, Bureau of Mines Reno (NV) Research Center.

NOTE.--See figure 3 for sample location.

*** APPENDIX C.--VLF-EM AND RADIOMETRIC MEASUREMENTS

Line 1400N				Line 1200 N				Line 1200 N - Cont.			
Station	Quad-rature	Dip angle ¹	Total cps	Station	Quad-rature	Dip angle ¹	Total cps	Station	Quad-rature	Dip angle ¹	Total cps
200E...	0	+10	90	400E...	0	+10	120	2800...	0	+5	110
	+1	+10	100		0	+10	120		0	+5	110
300....	+2	+10	110	500....	0	+10	150	2900...	+4	+10	110
	+1	+10	110		0	+10	150		+4	+10	110
400....	+2	+10	110	600....	0	+10	140	3000...	+4	+10	110
	0	+10	110		0	+10	130		+4	+10	110
500....	+2	+10	110	700....	0	+10	140	3100...	+2	+8	110
	0	+10	110		0	+10	140		0	+10	100
600....	+2	+12	110	800....	0	+10	120	3200...	0	+5	100
	0	+15	110		0	+10	150		+4	+10	100
700....	-2	+10	110	900....	0	+10	150	3300...	+4	+5	100
	0	+15	110		0	+12	160		+4	+5	60
800....	+4	+18	100	1000...	0	+12	150	3400...	+4	+5	110
	0	+18	110		0	+12	150		+4	+5	110
900....	0	+20	110	1100...	0	+17	150	3500...	+4	+5	100
	0	+20	110		0	+17	150		+4	+5	100
1000...	-2	+18	110	1200...	0	+17	150	3600...	+4	+5	100
	-2	+15	110		0	+12	150		+4	+5	100
1100...	+4	+15	110	1300...	0	+11	160	3700...	+4	+5	100
	+4	+10	100		0	+10	160		+6	+2	100
1200...	0	+10	100	1400...	0	+8	160	3800...	+2	+2	100
	0	+8	100		0	+10	160		+8	0	100
1300...	0	+7	100	1500...	0	+10	180	3900...	+4	0	100
	0	+5	110		0	+8	180		+4	0	100
1400...	0	+5	120	1600...	0	+8	180	4000...	0	+2	100
	0	+5	110		0	+5	180		+4	+5	100
1500...	0	+5	100	1700...	0	+5	180	4100...	+6	+2	100
	0	+5	110		-2	+5	190		+4	+3	80
1600...	0	+5	120	1800...	0	+8	180	4200...	+6	0	100
	0	+5	100		0	+8	180		+4	0	80
1700...	0	+5	100	1900...	-2	+8	180	4300...	+2	0	100
	+2	+5	100		-4	+5	180		+2	+2	80
1800...	0	+5	100	2000...	-2	+5	120	4400...	+2	0	100
	0	+5	100		-2	+5	120		+2	0	100
1900...	0	+5	100	2100...	-2	+5	120	4500...	+2	0	
	0	+5	100		-1	+5	130				
2000...	-2	+5	100	2200...	0	+5	100				
	0	+5	100		0	+5	100				
2100...	0	+5	80	2300...	0	+5	100				
	0	+5	100		0	+7	110				
2200...	0	+5	80	2400...	0	+5	110				
	0	+5	100		0	+5	110				
2300...	0	+5	100	2500...	0	+5	110				
	0	+5	100		0	+7	110				
2400...	0	+5	80	2600...	0	+7	110				
	0	+5	80		0	+5	110				
2500...	0	+5	100	2700...	0	+5	110				
					0	+5	110				

Line 1000 N			
Station	Quad-rature	Dip angle ¹	Total cps
00.....	+6	+10	140
	+4	+10	140
100E...	+6	+10	140
	+6	+10	120
200....	+10	+10	120
	+10	+10	120
300....	+10	+10	120
	+8	+10	150
400....	+8	+10	140
	+8	+8	140

See explanatory notes at end of table.

Line 600 N - Cont.				Line 600 N - Cont.				Line 400 N - Cont.			
Station	Quad- rature	Dip angle ¹	Total cps	Station	Quad- rature	Dip angle ¹	Total cps	Station	Quad- rature	Dip angle ¹	Total cps
400....	-4	+8	160	2800...	+4	+7	140	600....	+11	+25	180
	-4	+10	160		+5	+7	160		+10	+25	160
600....	-4	+12	180	2900...	+4	+5	200	700....	+8	+30	140
	-4	+12	210		+2	+5	200		+10	+25	140
600....	-2	+17	180	3000...	+2	+5	280	800....	0	+20	160
	+2	+18	160		+2	+10	300		+4	+25	230
700....	+2	+20	140	3100...	+2	+10	290	900....	+2	+22	200
	+6	+27	150		+1	+10	390		0	+20	220
800....	+2	+25	160	3200...	+1	+5	320	1000...	0	+25	220
	+2	+25	180		0	+7	400		0	+20	200
900....	-4	+23	200	3300...	0	+8	340	1100...	-2	+20	210
	-2	+25	230		0	+5	380		0	+20	200
1000...	-4	+25	180	3400...	+4	+8	400	1200...	+2	+18	200
	-4	+22	200		+4	+8	480		0	+18	200
1100...	+3	+25	220	3500...	+4	+8	410	1300...	0	+15	200
	+3	+20	220		+5	+8	430		+2	+17	190
1200...	+3	+20	220	3600...	+6	+8	430	1400...	+2	+15	190
	+4	+18	200		+6	+8	450		+4	+15	220
1300...	+4	+18	220	3700...	+6	+8	290	1500...	+4	+13	260
	+4	+15	230		+6	+4	360		+4	+15	220
1400...	+4	+15	250	3800...	+4	+4	280	1600...	+5	+12	300
	+4	+10	220		+4	+2	360		+2	+10	280
1500...	+18	+12	200	3900...	+4	+2	350	1700...	+2	+10	270
	+10	+10	220		+4	+2	320		+4	+10	240
1600...	+10	+10	220	4000...	+4	0	280	1800...	+6	+10	310
	+12	+10	280		+4	0	280		+8	+10	330
1700...	+10	+10	220	4100...	+4	0	320	1900...	+5	+10	350
	+8	+10	280		+4	0	300		+4	+8	300
1800...	0	+10	300	4200...	+4	0	140	2000...	+5	+8	260
	0	+10	350		+5	0	140		+2	+8	260
1900...	0	+10	340	4300...	+10	0	180	2100...	+2	+10	280
	0	+10	340		+6	-2	180		+4	+10	240
2000...	+2	+8	300	4400...	+8	-2	180	2200...	+4	+8	240
	+2	+10	200						+4	+8	180
2100...	+2	+10	270	Line 400 N				2300...	+1	+5	170
	-1	+10	290	Station	Quad- rature	Dip angle ¹	Total cps		0	+5	170
2200...	-1	+5	260	00.....	+4	0	140	2400...	+4	+10	180
	-1	+8	250		+0	0	140		0	+8	180
2300...	0	+5	210	100E...	+6	0	120	2500...	+4	+5	180
	+2	+8	210		+5	+5	120		0	+5	180
2400...	+2	+5	200	200....	-2	+5	120	2600...	0	+5	200
	+2	+5	180		0	+5	120		0	+5	180
2500...	+2	+5	200	300....	+1	+12	180	2700...	0	+5	380
	+2	+10	160		+4	+12	140		0	0	290
2600...	+4	+10	180	400....	+7	+15	250	2800...	+10	0	200
	+2	+10	190		+8	+20	240		+2	0	280
2700...	+2	+10	180	500....	+11	+20	170	2900...	-2	+3	380
	+3	+10	160		+6	+25	160		0	+10	420

See explanatory notes at end of table.

Line 00 - Cont.				Line 00 - Cont.				Line 00 - Cont.			
Station	Quad- rature	Dip angle ¹	Total cps	Station	Quad- rature	Dip angle ¹	Total cps	Station	Quad- rature	Dip angle ¹	Total cps
200....	+4	+10	140	2200...	0	+10	180	4600...	+12	-8	140
	+4	+8	120		+3	+8	260		+13	-5	140
100....	+2	+8	120	2300...	+4	+5	300	4700...	+10	-5	160
	+6	+12	120		+4	+8	280		+6	0	150
00.....	+12	+15	180	2400...	+5	+8	300	4800...	+8	0	150
	+20	+15	200		-2	+7	290	Line 200S			
100E...	+20	+20	200	2500...	-2	+10	300	Station	Quad- rature	Dip angle ¹	Total cps
	+24	+20	150		-4	+7	300	600W...	+10	+10	100
200....	+24	+20	80	2600...	+2	+5	300		+10	+10	80
	+14	+20	120		0	+5	300	500....	+12	+10	100
300....	+18	+20	160	2700...	+5	+5	350		+8	+10	100
	+18	+20	140		+8	0	310	400....	+8	+7	120
400....	+20	+20	280	2800...	+8	+6	310		+6	0	140
	+4	+20	280		+4	+5	290	300....	+6	+2	120
500....	+8	+20	210	2900...	-2	+5	260		+4	+5	120
	+7	+20	200		+2	+6	280	200....	+4	+5	120
600....	+4	+20	150	3000...	+4	+4	310		+4	+8	120
	+2	+20	180		+6	+5	260	100....	+10	+5	110
700....	+3	+18	180	3100...	+4	+5	250		+10	+15	100
	0	+20	150		+2	+8	250	00.....	+16	+15	120
800....	+2	+20	170	3200...	+10	+5	250		+20	+20	110
	+6	+20	180		+8	+7	280	100E...	+24	+25	140
900....	+2	+20	150	3300...	+6	+5	300		+20	+25	140
	+6	+18	440		+4	+5	260	200....	+20	+25	140
1000...	0	+18	200	3400...	+8	+4	330		+24	+22	140
	-2	+15	180		+8	+2	220	300....	+18	+20	140
1100...	+6	+15	220	3500...	+10	0	210		+18	+20	160
	+4	+15	200		+12	+5	220	400....	+18	+20	140
1200...	+3	+12	200	3500...	+14	0	260		+16	+22	140
	+3	+15	200		+14	+4	250	500....	+16	+20	140
1300...	0	+15	200	3700...	+8	0	200		+16	+20	150
	0	+15	210		+8	+4	220	600....	+16	+20	210
1400...	0	+15	250	3800...	+8	0	280		+8	+20	210
	+4	+12	250		+10	+2	240	700....	+4	+15	240
1500...	+2	+12	260	3900...	+10	+2	300		-6	+15	210
	+2	+10	270		+10	0	260	800....	0	+15	250
1600...	0	+12	280	4000...	+12	+2	240		-8	+20	180
	+3	+12	280		+10	0	240	900....	-8	+20	180
1700...	+6	+10	250	4100...	+8	-2	240		-4	+15	300
	+3	+12	270		+4	0	240	1000...	-4	+15	140
1800...	+4	+10	250	4200...	+12	-5	250		-2	+18	220
	+5	+13	280		+13	-2	310	1100...	-2	+17	180
1900...	+3	+8	180	4300...	+14	-2	220		-2	+17	180
	0	+10	170		+14	-5	220	1200...	+2	+16	180
2000...	0	+10	160	4400...	+8	-2	220		+4	+12	180
	+4	+10	160		+12	-5	240	1300...	0	+15	180
2100...	-2	+8	170	4500...	+12	-10	170		0	+15	220
	+3	+8	180		+12	-10	140		+3	+10	220
									0	+12	200

See explanatory notes at end of table.

Line 200 S - Cont.				Line 200 S - Cont.				Line 400 S - Cont.			
Station	Quad- rature	Dip angle ¹	Total cps	Station	Quad- rature	Dip angle ¹	Total cps	Station	Quad- rature	Dip angle ¹	Total cps
1400...	0	+10	240	3800...	+14	+5	220	1000...	0	+15	200
	+2	+15	250		+10	5	300		+4	+15	210
1500...	0	+12	250	3900...	+10	+2	320	1100...	0	+15	210
	+4	+10	220		+12	0	280		0	+15	240
1600...	0	+10	220	4000...	+3	+5	260	1200...	0	+10	280
	0	+12	230		+10	0	280		-2	+12	200
1700...	+2	+12	180	4100...	+6	0	240	1300...	-2	+10	180
	+2	+12	180		+6	0	260		-2	+10	160
1800...	0	+10	190	4200...	+10	0	250	1400...	-3	+10	180
	+5	+12	200		+12	0	290		+4	+12	180
1900...	+5	+12	200	4300...	+12	0	250	1500...	+3	+12	220
	+5	+12	200		+10	0	240		+3	+10	180
2000...	+2	+12	280	4400...	+10	0	200	1600...	+2	+12	160
	+2	+12	220		+8	0	240		+4	+12	200
2100...	0	+10	300	4500...	+10	0	220	1700...	+4	+10	200
	-2	+7	220		+10	0	450		+2	+10	220
2200...	-3	+10	220	Line 400S				1800...	+2	+12	180
	+2	+8	240	Station	Quad- rature	Dip angle ¹	Total cps		0	+15	180
2300...	+2	+10	260	400W...	+10	+10	120	1900...	0	+10	200
	+4	+8	280		+8	+12	120		0	+10	120
2400...	0	+8	350	300....	+4	+12	140	2000...	0	+12	140
	+2	+8	280		+18	+15	150		+1	+12	140
2500...	+4	+7	320	200....	+13	+15	120	2100...	+1	+12	140
	+4	+5	250		+16	+20	120		+1	+10	160
2600...	+4	+5	250	100....	+9	+20	140	2200...	0	+12	180
	+6	+5	300		+16	+20	140		0	+10	160
2700...	0	+5	220	00.....	+14	+20	140	2300...	0	+10	160
	+4	+5	220		+12	+15	150		0	+10	150
2800...	0	+5	280	100E...	+10	+15	120	2400...	0	+10	180
	-2	+5	250		+10	+20	100		+6	+5	200
2900...	0	+2	300	200....	+14	+20	120	2500...	+8	+5	200
	-2	+2	280		+14	+15	140		+8	+7	210
3000...	0	+2	280	300....	+10	+20	140	2600...	+6	+5	220
	0	+2	220		+10	+20	100		+8	+5	180
3100...	0	+2	280	400....	+8	+20	150	2700...	+8	+5	180
	+2	+2	230		+18	+20	150		+9	+10	180
3200...	+6	+4	250	500....	+10	+20	160	2800...	+4	+5	220
	+8	+2	220		+14	+15	160		+4	+5	200
3300...	+12	+2	180	600....	+14	+15	160	2900...	+4	+5	230
	+14	+2	200		+14	+15	160		+4	+5	260
3400...	+14	+2	220	700....	+4	+15	160	3000...	+4	+5	230
	+10	+5	250		+2	+15	240		+4	+2	280
3500...	+12	+4	220	800....	+6	+15	240	3100...	+2	0	280
	+8	+5	240		+3	+15	250		+2	+2	320
3600...	+10	+5	240	900....	+6	+15	200	3200...	+8	0	280
	+6	+2	240		+4	+15	210		+4	0	300
3700...	+8	+5	260					3300...	+4	0	280
	+14	+2	300						+4	+2	250

See explanatory notes at end of table.

Line 400 S - Cont.			
Station	Quad-rature	Dip angle ¹	Total cps
3400...	+4	+5	270
	+2	0	280
3500...	+4	+2	240
	+4	+5	300
3600...	0	+5	220
	0	+5	250
3700...	0	+5	220
	0	+5	220
3800...	+10	+5	220
	+8	+5	300
3900...	+8	+5	300
	+6	+5	300
4000...	+6	0	290
	+8	0	270
4100...	+4	+5	270
	+4	0	280
4200...	0	0	500
	+10	0	550
4300...	+8	0	680
	+8	0	600
4400...	+2	0	400
	+2	0	500
4500...	+2	0	340

Line 600 S			
Station	Quad-rature	Dip angle ¹	Total cps
300W...	+12	+12	140
	+12	+12	140
200....	+12	+12	140
	+20	+20	140
100....	+10	+10	140
	+10	+10	140
00.....	+16	+16	160
	+16	+16	150
100E...	+16	+16	150
	+10	+10	150
200....	+20	+20	180
	+12	+12	190
300....	+8	+8	160
	+8	+8	150
400....	+6	+6	200
	+8	+8	200
500....	+8	+8	190
	+4	+17	210
600....	+6	+15	210
	+6	+15	200
700....	0	+18	180
	+2	+18	200

Line 600 S - Cont.			
Station	Quad-rature	Dip angle ¹	Total cps
800....	0	+17	210
	+2	+15	200
900....	+4	+12	200
	+2	+15	190
1000...	0	+12	180
	+2	+12	150
1100...	+6	+14	160
	+6	+14	140
1200...	+6	+12	120
	+6	+12	140
1300...	+6	+10	140
	+6	+12	120
1400...	+6	+12	190
	+4	+12	120
1500...	+6	+10	160
	+4	+10	180
1600...	+4	+10	80
	+6	+12	90
1700...	+4	+12	80
	+6	+12	80
1800...	+6	+12	120
	+6	+12	100
1900...	+6	+12	100
	+6	+12	100
2000...	+6	+12	150
	+4	+8	160
2100...	+4	+10	180
	+4	+10	120
2200...	+4	+10	190
	+2	+8	200
2300...	0	+12	150
	+4	+12	190
2400...	+2	+10	150
	0	+10	170
2500...	+6	+10	170
	+6	+8	170
2600...	+6	+5	170
	+6	+5	220
2700...	+6	+5	180
	+8	+2	180
2800...	+8	+2	180
	+10	+2	150
2900...	+10	+2	200
	+2	0	180
3000...	+4	+5	200
	+4	+2	180
3100...	+6	+2	170
	+6	0	180

Line 600 S - Cont.			
Station	Quad-rature	Dip angle ¹	Total cps
3200...	+6	0	190
	+4	0	180
3300...	+4	+2	230
	+4	+2	200
3400...	+4	+2	200
	+4	+5	220
3500...	+4	+5	240
	+4	+5	300
3600...	+10	+5	250
	+8	+5	320
3700...	+6	+5	360
	+4	+5	310
3800...	+4	+5	310
	+6	+5	300
3900...	+6	+5	320
	+8	+4	380
4000...	+4	+2	280
	+4	0	240
4100...	+8	+5	220
	+4	0	200
4200...	+6	0	180
	+4	0	220
4300...	+6	+4	140
	+4	+5	140
4400...	+4	+5	120

Line 800 S			
Station	Quad-rature	Dip angle ¹	Total cps
300W...	+4	+16	180
	+4	+15	160
200....	+6	+15	160
	+6	+17	160
100....	+8	+20	180
	+8	+20	190
00.....	+6	+20	180
	+4	+20	160
100E...	+8	+20	160
	+12	+20	160
200....	+14	+20	150
	+18	+18	140
300....	+12	+15	140
	+12	+15	140
400....	+14	+15	160
	+6	+15	160
500....	+6	+12	160
	+6	+12	160
600....	+10	+12	150
	+8	+12	150

See explanatory notes at end of table.

Line 800 S - Cont.				Line 800 S - Cont.				Line 1000 S - Cont.			
Station	Quad- rature	Dip angle ¹	Total cps	Station	Quad- rature	Dip angle ¹	Total cps	Station	Quad- rature	Dip angle ¹	Total cps
700....	-2	+15	160	3100...	+8	0	210	800....	-12	+18	180
	-8	+15	160		+8	0	200		-8	+18	160
800....	-6	+15	220	3200...	0	+5	190	900....	-8	+12	140
	-4	+18	220		0	+5	190		-10	+18	180
900....	-4	+18	180	3300...	+10	0	220	100....	-2	+18	160
	-4	+20	130		+10	0	200		+6	+18	180
1000...	0	+20	150	3400...	+10	+2	220	1100...	+10	+15	160
	0	+12	120		+2	0	260		+10	+15	140
1100...	0	+15	100	3500...	+4	+2	260	1200...	+10	+20	110
	0	+15	140		+2	0	480		+10	+15	120
1200...	0	+10	120	3600...	+2	0	350	1300...	+10	+18	110
	0	+10	100		+4	0	380		+8	+15	120
1300...	0	+10	90	3700...	+5	0	430	1400...	+6	+12	100
	+2	+12	80		+4	0	430		+10	+10	100
1400...	+4	+12	90	3800...	+6	+2	300	1500...	+10	+10	100
	+4	+12	80		+8	0	290		+4	+10	80
1500...	+4	+10	60	3900...	+8	0	330	1600...	+4	+10	60
	+4	+10	60		+4	0	340		+4	+10	100
1600...	+4	+10	60	4000...	+4	0	340	1700...	+4	+10	100
	+4	+10	60		+4	+5	300		+6	+10	100
1700...	+4	+10	60	4100...	+10	+5	280	1800...	+8	+10	100
	+4	+10	60		+2	+3	260		+4	+10	80
1800...	+4	+12	50	4200...	+2	0	200	1900...	+4	+10	80
	+10	+10	50		+2	0	160		+4	+10	80
1900...	+4	+10	50	4300...	+2	+2	140	2000...	+6	+8	90
	+4	+10	50		+4	0	100		+6	+10	90
2000...	+4	+10	110	4400...	+4	0	100	2100...	+8	+10	90
	+4	+10	80		+4	0	100		+8	+10	90
2100...	+4	+12	80	4500...	+4	0	100	2200...	+10	+10	100
	+4	+10	80						+10	+10	90
2200...	+4	+10	80	Line 1000 S				2300...	+10	+8	100
	+4	+10	80	Station	Quad- rature	Dip angle ¹	Total cps		+10	+10	100
2300...	+4	+10	90	00.....	+8	+16	140	2400...	+10	+10	100
	+4	+8	90		+8	+15	150		+6	+10	100
2400...	+4	+8	100	100E...	+11	+14	140	2500...	+6	+8	100
	+4	+8	120		+8	+15	140		+2	+10	100
2500...	+4	+8	120	200....	+6	+15	120	2600...	+2	+5	100
	+4	+8	120		+6	+15	120		+2	+2	100
2600...	+4	+8	140	300....	+6	+15	120	2700...	+2	+5	100
	+4	+8	150		+4	+15	120		+4	+2	120
2700...	+8	+5	170	400....	+4	+18	150	2800...	+2	0	150
	+10	+2	180		+10	+20	140		+2	+2	130
2800...	+6	+3	160	500....	+10	+20	140	2900...	0	+2	150
	+6	+2	160		+10	+18	140		0	0	180
2900...	+6	+2	180	600....	+10	+16	120	3000...	+2	0	180
	+6	0	190		+12	+15	150		+2	0	190
3000...	+4	0	190	700....	0	+18	190	3100...	+2	0	200
	+6	0	200		-10	+18	190		+2	+2	190

See explanatory notes at end of table.

Line 1000 S - Cont.			
Station	Quad- rature	Dip angle ¹	Total cps
3200...	+4	+2	180
	0	+2	150
3300...	0	+5	180
	+3	0	200
3400...	+2	0	200
	+2	0	180
3500...	+2	0	200
	+3	0	210
3600...	+3	0	240
	+2	0	330
3700...	+2	0	380
	+2	+2	430
3800...	+2	+2	350
	0	+5	300
3900...	+6	+2	330
	+8	+4	330
4000...	+8	+2	380
	+8	+5	380
4100...	0	+5	300
	0	+5	300
4200...	0	+2	220
	+2	+2	280
4300...	+2	0	120
	+2	0	120
4400...	+4	0	130
	+4	0	100
4500...	+4	0	100

Line 1200 S - Cont.			
Station	Quad- rature	Dip angle ¹	Total cps
800....	+4	+12	140
	+6	+12	180
900....	+10	+12	220
	+10	+15	140
1000...	+10	+15	190
	+8	+12	160
1100...	-4	+10	150
	-2	+10	160
1200...	-2	+10	180
	-2	+10	140
1300...	-2	+10	140
	0	+10	140
1400...	0	+10	100
	0	+10	100
1500...	+10	+10	100
	+8	+10	100
1600...	+6	+10	100
	+6	+10	100
1700...	0	+10	100
	0	+12	120
1800...	+6	+10	120
	+10	+10	100
1900...	+10	+10	100
	+10	+10	100
2000...	+8	+10	100
	+4	+8	100
2100...	+6	+10	100
	+8	+10	100
2200...	+5	+10	100
	+6	+10	120
2300...	+8	+8	100
	+6	+8	120
2400...	+4	+8	100
	+4	+8	100
2500...	+6	+8	80
	+5	+5	100
2600...	+4	+5	100
	+4	+5	80
2700...	+10	+5	110
	+4	+5	100
2800...	+4	+8	100
	+6	+4	120
2900...	+8	0	120
	+6	0	150
3000...	+2	+5	140
	+4	+5	150
3100...	+2	+5	180
	+2	0	160

Line 1200 S - Cont.			
Station	Quad- rature	Dip angle ¹	Total cps
3200...	+2	0	150
	+4	0	160
3300...	+2	0	140
	+2	0	150
3400...	+4	0	180
	+6	0	240
3500...	+6	0	200
	+8	0	150
3600...	+4	0	280
	+8	0	240
3700...	+4	0	240
	+4	+2	240
3800...	+11	0	220
	+4	+5	240
3900...	+6	+4	260
	+4	+2	220
4000...	+8	+2	240
	+12	0	200
4100...	+10	0	200
	0	0	150
4200...	+5	+5	150
	+8	0	100
4300...	+6	0	140
	+7	0	120
4400...	+8	0	120

Line 1200 S			
Station	Quad- rature	Dip angle ¹	Total cps
100W...	0	+15	100
	+2	+15	80
00.....	0	+15	100
	0	+18	100
100E...	0	+15	120
	+2	+16	100
200....	0	+15	80
	+2	+15	100
300....	0	+15	120
	0	+15	140
400....	0	+15	120
	+6	+12	140
500....	0	+12	220
	-2	+12	160
600....	+4	+15	220
	+6	+15	240
700....	+6	+10	140
	+6	+10	180

Line 1400 S			
Station	Quad- rature	Dip angle ¹	Total cps
2400E..	+2	+5	100
	+5	+5	100
2500...	+4	+5	100
	+2	+5	100
2600...	+10	+5	100
	+10	+6	100
2700...	+10	+5	100
	+8	+5	110
2800...	+10	+5	110
	+6	+7	120
2900...	+12	+8	120
	+10	+8	140
3000...	+8	+8	140
	+6	+7	160
3100...	+4	+7	150
	+4	+7	200
3200...	+4	+7	180
	+4	+7	200
3300...	+2	+7	180
	+6	+7	200

See explanatory notes at end of table.

Line 1400 S - Cont.				Line 1600 S				Line 1600 S - Cont.			
Station	Quad-rature	Dip angle ¹	Total cps	Station	Quad-rature	Dip angle ¹	Total cps	Station	Quad-rature	Dip angle ¹	Total cps
3400...	+4	+7	300	2400E..	+4	+10	150	3500...	0	+7	120
	+2	+7	240		+8	+5	150		0	+8	110
3500...	+2	+7	300	2500...	+6	+10	120	3600...	0	+10	140
	+2	+4	200		+5	+10	120		0	+10	120
3600...	+4	+5	150	2600...	+5	+5	130	3700...	+2	+10	110
	+2	+10	200		+5	+5	140		+2	+10	110
3700...	+2	+10	180	2700...	+4	+8	120	3800...	+2	+10	110
	+3	+8	160		+4	+5	130		+4	+10	100
3800...	+4	+5	150	2800...	+3	+10	120	3900...	+2	+8	100
	+4	+7	160		+10	+20	190		+2	+8	110
3900...	+4	+7	270	2900...	+6	+20	180	4000...	+8	+8	200
	0	+7	210		+6	+12	210		+5	+7	200
4000...	-4	+6	200	3000...	+8	+10	220	4100...	+5	+8	100
	-4	+5	210		+4	+10	200		+5	+8	80
4100...	-4	+5	280	3100...	+4	+15	160	4200...	+5	+8	80
	+3	+7	210		+6	+10	180		+5	+8	80
4200...	-3	+7	180	3200...	+4	+8	170	4300...	+5	+8	80
	-2	+7	100		+4	+7	180		+5	+8	80
4300...	0	+7	180	3300...	+4	+7	120	4400...	+5	+8	80
	0	+7	120		+4	+8	110		+4	+8	80
4400...	0	+7	80	3400...	+8	+7	110	4500...	+5	+8	80
	+2	+7	100		0	+7	120				
4500...	0	+6	90								

W West.

E East.

¹All readings taken facing west.

NOTE.--See figures 3, 8, and 9 for survey grid and contouring.